AFRL-VS-HA-TR-2004-1031

IMPROVED FOCAL DEPTH DETERMINATION FOR USE IN SEISMIC MONITORING OF THE UNDERGROUND NUCLEAR EXPLOSIONS

J. R. Murphy
B. W. Barker
M. E. Marshall
W. L. Rodi

Science Applications International Corporation
10260 Campus Point Drive
San Diego, CA 92121-1578

19 November 2003

Final Report

20040518 089

APPROVED FOR PUBLIC RELEASE; DISTRIBUTON UNLIMITED

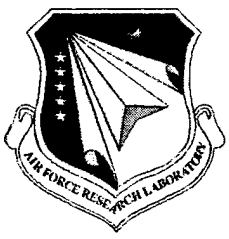

AIR FORCE RESEARCH LABORATORY
Space Vehicles Directorate
29 Randolph Rd
AIR FORCE MATERIEL COMMAND
Hanscom AFB, MA 01731-3010

This technical report has been reviewed and is approved for publication.

/SIGNED/	/SIGNED/
ROBERT RAISTRICK Contract Manager	ROBERT BELAND Branch Chief

This document has been reviewed by the ESC Public Affairs Office and has been approved for release to the National Technical Information Service (NTIS).

Qualified requestors may obtain additional copies from the Defense Technical Information Center (DTIC). All others should apply to the NTIS.

If your address has changed, if you with to be removed from the mailing list, or if the addressee is no longer employed by your organization, please notify AFRL/VSIM, 29 Randolph Rd., Hanscom AFB, MA 01731-3010. This will assist us in maintaining a current mailing list.

Do not return copies of this report unless contractual obligations or notices on a specific document require that it be returned.

REPORT DOCUMENTATION PAGE

Form Approved OMB No. 0704-0188

Public reporting burden for this collection of information is estimated to average 1 hour per response, including the time for reviewing instructions, searching existing data sources, gathering and maintaining the data needed, and completing and reviewing this collection of information. Send comments regarding this burden estimate or any other aspect of this collection of information, including suggestions for reducing this burden to Department of Defense, Washington Headquarters Services, Directorate for Information Operations and Reports (0704-0188), 1215 Jefferson Davis Highway, Suite 1204, Arlington, VA 22202-4302. Respondents should be aware that notwithstanding any other provision of law, no person shall be subject to any penalty for failing to comply with a collection of information if it does not display a currently valid OMB control number. **PLEASE DO NOT RETURN YOUR FORM TO THE ABOVE ADDRESS.**

1. REPORT DATE *(DD-MM-YYYY)* 19-11-2003	**2. REPORT TYPE** FINAL
3. DATES COVERED *(From - To)* 26 Sep 01 - 28 Nov 03	
4. TITLE AND SUBTITLE Improved Focal Depth Determination for Use in Seismic Monitoring of Underground Nuclear Explosions	**5a. CONTRACT NUMBER** DTRA01-01-C-0056
	5b. GRANT NUMBER
	5c. PROGRAM ELEMENT NUMBER
6. AUTHOR(S) J. R. Murphy, B. W. Barker, M. E. Marshall and W. L. Rodi	**5d. PROJECT NUMBER** DTRA
	5e. TASK NUMBER OT
	5f. WORK UNIT NUMBER A1
7. PERFORMING ORGANIZATION NAME(S) AND ADDRESS(ES) Science Applications International Corporation 10260 Campus Point Drive San Diego, CA 92121-1578	**8. PERFORMING ORGANIZATION REPORT NUMBER**
9. SPONSORING / MONITORING AGENCY NAME(S) AND ADDRESS(ES) Air Force Research Laboratory 29 Randolph Road Hanscom AFB MA 01731-3010	**10. SPONSOR/MONITOR'S ACRONYM(S)** AFRL/VSBYE
	11. SPONSOR/MONITOR'S REPORT NUMBER(S) AFRL-VS-HA-TR-2004-1031

12. DISTRIBUTION / AVAILABILITY STATEMENT

Approved for Public Release; Distribution Unlimited

13. SUPPLEMENTARY NOTES

14. ABSTRACT

Seismic event location remains as one of the most important discriminants for separating natural tectonic and explosive events. For example, it has been estimated that approximately 80%of known global earthquakes have focal depths greater than 50 km or are located more than 25 km at sea. Since underwater nuclear explosions can be confidently identified to very low yields using hydroacoustic data, it follows that the vast majority of earthquakes can potentially be identified on the basis of location alone. This is an important observation since global monitoring of underground nuclear testing may require the screening of tens of thousands of seismic events per year and, in order to perform this function efficiently, it will be necessary to have simple and robust discriminants available which can be used to eliminate the vast majority of these events from more detailed consideration. However, in order to be useful for such discrimination purposes, the uncertainties associated with seismic locations must be well defined and reliable and this has proved to be difficult to accomplish.

15. SUBJECT TERMS

Seismic discrimination Seismic sources Yield

16. SECURITY CLASSIFICATION OF:			**17. LIMITATION OF ABSTRACT**	**18. NUMBER OF PAGES**	**19a. NAME OF RESPONSIBLE PERSON**
a. REPORT	**b. ABSTRACT**	**c. THIS PAGE**			Robert Raistrick
UNCLAS	UNCLAS	UNCLAS	SAR		**19b. TELEPHONE NUMBER** *(include area code)* 781 377-3726

TABLE OF CONTENTS

FIGURES

SECTION 1

INTRODUCTION

Seismic event location remains as one of the most important discriminants for separating natural tectonic and explosive events. For example, it has been estimated that approximately 80% of known global earthquakes have focal depths greater than 50 km or are located more than 25 km at sea. Since underwater nuclear explosions can be confidently identified to very low yields using hydroacoustic data, it follows that the vast majority of earthquakes can potentially be identified on the basis of location alone. This is an important observation, since global monitoring of underground nuclear testing may require the screening of tens of thousands of seismic events per year and, in order to perform this function efficiently, it will be necessary to have simple and robust discriminants available which can be used to eliminate the vast majority of these events from more detailed consideration. However, in order to be useful for such discrimination purposes, the uncertainties associated with seismic locations must be well-defined and reliable; and this has proven to be difficult to accomplish to the required degree of accuracy.

More specifically, high confidence estimation of focal depths remains as an outstanding seismic monitoring problem. If accurate focal depths could be determined for the majority of earthquakes deeper than 5, or even 10 km, the event screening problem would be much easier. However, despite intensive efforts by well-trained and experienced analysts, more than two-thirds of the GSETT-3 REB events were assigned artificially constrained depths. Moreover, the cited accuracies of even those relatively few focal depth estimates is open to serious question, particularly in the light of the evidence that the corresponding epicentral

uncertainties appear to be significantly underestimated by the current hypocentral location algorithm. Thus, for example, Fisk et al (2000) found a number of cases in the GSETT-3 database where the cited uncertainties in the focal depths of earthquakes in particular areas had been consistently underestimated by the PIDC location program. Such discrepancies are frequently compensated for in a crude fashion by artificially inflating the input variance values until the associated confidence bounds encompass the required percentage of verified values. This was the interim approach taken by Fisk et al (2000) in their formulation of the focal depth discriminant for the experimental event screening system at the IDC. However, this is an ad hoc procedure which can potentially lead to serious focal depth estimation errors under previously untested conditions.

This lack of a reliable measure of focal depth uncertainty has a number of important ramifications with respect to event screening. That is, not only does it reduce the effectiveness of the focal depth discriminant itself, but it also has implications for some of the other standard discriminants. This follows from the fact that from a seismic monitoring perspective, if an event can't be confidently shown to have significant focal depth, it must be assumed to be shallow enough to be considered as a possible explosion. For this reason, the default focal depth typically employed in seismic monitoring of explosions is zero, as opposed to the 33 km value frequently employed by NEIS. Now if events which are actually subcrustal are assigned shallow focal depths, this can have a pronounced effect on the utility of other discriminants, such as M_s/m_b. For example, it has been shown that deep, subcrustal earthquakes generally show explosion-like M_s-m_b values (i.e., M_s-$m_b < -1.0$), in accord with the theoretically expected decrease in M_s with increasing focal depth. It follows that, if events which are actually subcrustal have to be analyzed under the assumption that they are shallow, the effectiveness of the

Ms/mb discriminant will be greatly reduced. Thus, any improvements that can be made in focal depth determination capability will have significant and multiple implications with respect to operational monitoring capability.

This report presents a summary of a variety of investigations conducted under this contract that have been directed toward the development of improved procedures for estimating focal depths of seismic sources. The utility of the secondary depth phases pP and sP is addressed in Section 2, where the various factors affecting depth phase identification are discussed and illustrated; and a network beamforming procedure for use in the automatic identification of candidate depth phases is described and applied to seismic data recorded from large samples of Hindu Kush, Honshu, Hokkaido and Lop Nor earthquakes. In Section 3 we discuss the use of the F detector as a tool to assist in determining the validity of candidate depth phases. This is followed in Section 4 with an assessment of the use of calibrated S-P differential arrival time information to provide independent estimates of event origin time for use as constraints in the hypocenter location process. The report concludes with Section 5, which contains a short summary and statement of conclusions regarding improvements in focal depth determination for use in the seismic monitoring of underground nuclear explosions.

SECTION 2

IMPROVED DETECTION AND IDENTIFICATION OF SECONDARY DEPTH PHASES

2.1 BACKGROUND.

Reliable identification of the depth phases pP and sP provides one of the strongest pieces of evidence that a seismic event is a naturally occurring earthquake when the time delay between pP and direct P exceeds about three seconds, implying a focal depth of greater than 10 km. However, confident identification of such phases on actual recordings is not always a simple matter. That is, it is first necessary to unambiguously identify a phase onset in the P coda background; and it is then required to confirm that this phase is actually a depth phase and not some other P phase, such as PcP, which might have an expected arrival time within the time window being analyzed. Thus, with regard to secondary phase detection, analysts are generally required to verify that the phase amplitude is several times the P coda background before it can be accepted for consideration as a possible depth phase. For positive identification as a depth phase, it is generally further required that the subject arrival be detected at several stations at different epicentral distances and that the time interval between its onset time and the associated P onset time be an increasing function of epicentral distance. This distance dependence is commonly referred to as "step-out," and the IASPEI 91 travel time tables predict step-outs between 30 and 90 degrees of approximately 0.4 seconds for a focal depth of 15 km, 4.4 seconds for a focal depth of 100 km and 13.7 seconds for a focal depth of 300 km. Thus, even with high quality data for which it is possible to determine pP-P time of arrival differences with an accuracy

of about 1 second, it is generally not possible to apply the step-out identification criterion to pP for events with focal depth less than about 50 km. Unfortunately, it was discovered during the course of the GSETT-3 that it is not an easy matter to specify analyst review procedures which will assure such high confidence identification of depth phases on a routine basis. For example, Figure 2-1 shows ARCES and NORES data recorded from the Hindu Kush earthquake of 1997/02/22, with annotated analyst pP picks which were used to estimate a very precise focal depth for this event. It can be seen that, while there is evidence of energy arriving near the picked pP times at both these stations, the arrivals do not appear to be distinctively different from the preceding P coda; and their

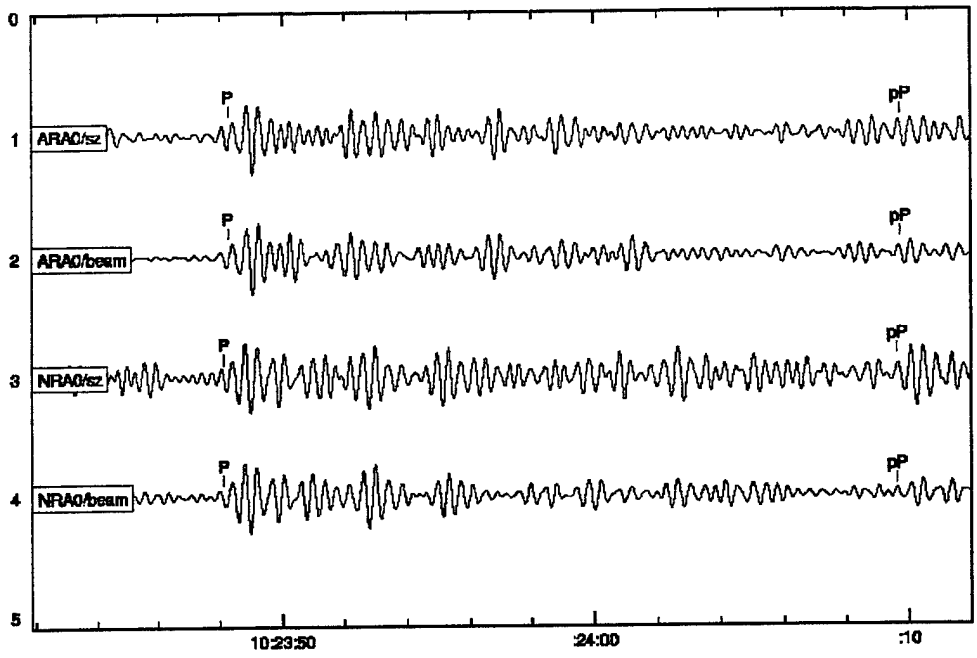

Figure 2-1. Center element seismograms (sz) and infinite velocity beams (beam) corresponding to the ARCES and NORES recordings of the 1997/02/22 Hindu Kush earthquake showing the analyst picked arrival times for P and pP.

identification would have to be considered to be highly questionable in the absence of further corroborative evidence, such as moveout. However, the moveout criterion can not be applied in this case due to the proximity of the two stations; and, consequently, these analyst picks would have to be rejected as unconfirmed for event screening purposes. A similar example is shown in Figure 2-2 for the Hindu Kush earthquake of 1997/09/11. In this case, there are three reported pP observations over the epicentral distance range extending from 18 to 73 degrees, which do show some indication of moveout. However, once again, identification of the picked phases on the recorded waveforms appears to be problematic in that there are no obvious distinct arrivals at the analyst picked pP times at any of the three stations. Experimentation with different frequency filters

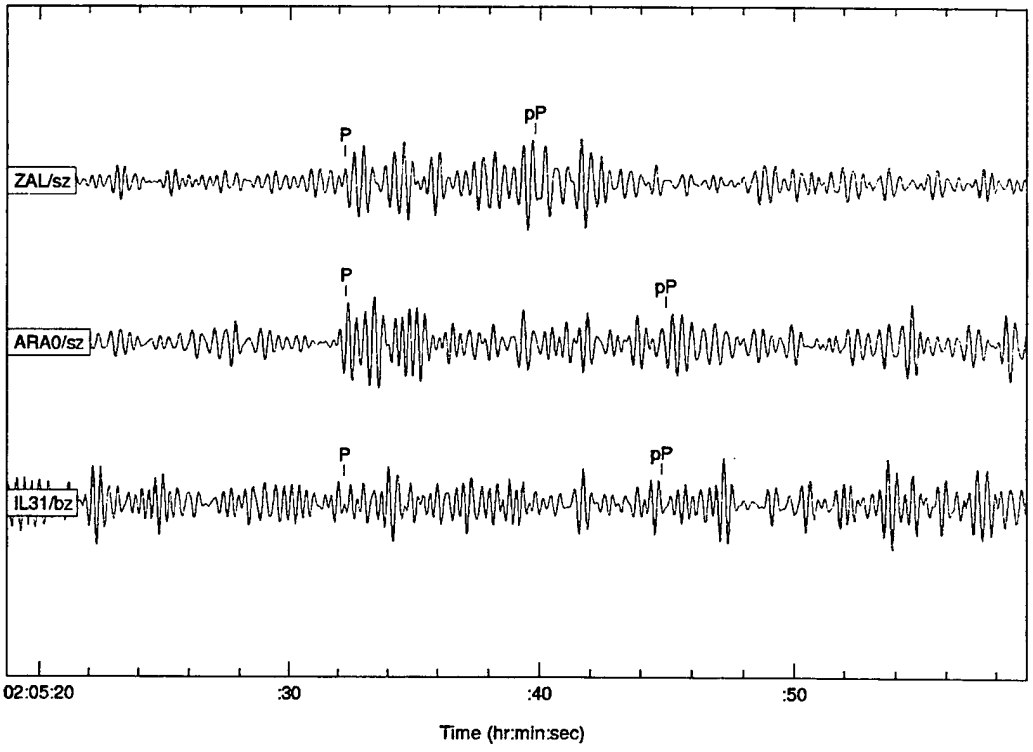

Figure 2-2. Single component seismograms corresponding to the ZAL, ARCES and ILAR recordings of the 1997/09/11 Hindu Kush earthquake showing the analyst picked arrival times for P and pP.

and array beams produced no better results, leading to the conclusion that these are also false detections. There are also numerous examples in the GSETT-3 database of the converse problem, in which the analyst failed to identify fairly obvious depth phases, leading to inferior estimates of focal depth. Such examples indicate that improved tools are needed to help the analyst to improve on the detection and identification of the depth phases pP and sP.

Leaving aside for the moment the various types of analyst errors that can occur, it is important to address the more general question of why depth phase identification continues to be such a difficult problem despite all the advances in instrumentation and signal processing which have been implemented in recent years. For example, during the GSETT-3 experiment, approximately 2/3 of the events reported in the REB had depths artificially constrained to the surface; and, of the remaining 1/3 of the events which were assigned free depths, only about 20% were determined on the basis of depth phase data. That is, depth phase data were reported for only about 5% of the total number of REB events. There are a number of factors which contribute to these low levels of detectability. An obvious one is that, for the many shallow events, the time separation between pP and P may be so short in some cases that the pP arrival is obscured by the P coda, particularly for earthquakes with complex source functions. However, the problem persists for deeper events for a variety of more subtle reasons. We will illustrate some of these complicating effects using data recorded from REB events in the Hindu Kush region of Asia. Because of the tectonics in this region, numerous events in the depth range 200 to 250 km occur in close proximity to one another, providing a convenient data set to illustrate depth phase variability. The first effect to be considered is associated with the fact that the direct P and surface reflected pP and sP phases do not travel exactly the same paths from the source to the receiver; and, consequently, their

pulse shapes can appear to be quite different. More specifically, the surface reflected phases propagate up to the surface and back through the attenuative surface layers above the source, which results in surface reflected pulses which are typically of lower dominant frequency than the associated direct P pulses. This effect is illustrated in Figure 2-3 using data recorded at three nearby North American stations from the Hindu Kush earthquake of 1997/01/10. Note that the dominant frequency content of pP is lower than that of P on the broadband signals (left) and that the pP/P amplitude ratios show significant variability among these three stations located in the same narrow azimuth window. However, when these same signals are lowpass filtered below 1.5 Hz (right), it can be seen that the pP/P amplitude ratios become much more similar, confirming the fact that the large variability observed on the broadband traces is due to differences in dominant frequency content between the P and pP signals observed at these stations. Such differences contribute to the difficulty in correlating depth phase arrivals between different stations. A second factor which complicates the depth phase identification process is earthquake focal mechanism which can also produce large variations in signal characteristics between stations for a given event and between events at a given station. Such effects are illustrated in Figure 2-4 which shows bandpass filtered (1-2 Hz) recordings for station MBC in Canada from a series of nearby Hindu Kush earthquakes with depths in the 200 to 250 km range. Note the order of magnitude variations in the pP/P and sP/P amplitude ratios which are presumably associated with variations in focal mechanism between these closely spaced events. More surprising is the fact that such variability in focal mechanism between nearby events can be large enough in some cases to produce consistent differences in pP/P amplitude ratios at large numbers of widely separated stations. An example of this type of variability is shown in Figure 2-5 using recordings at the same stations from two nearby Hindu Kush earthquakes with comparable focal depth (i.e. 208

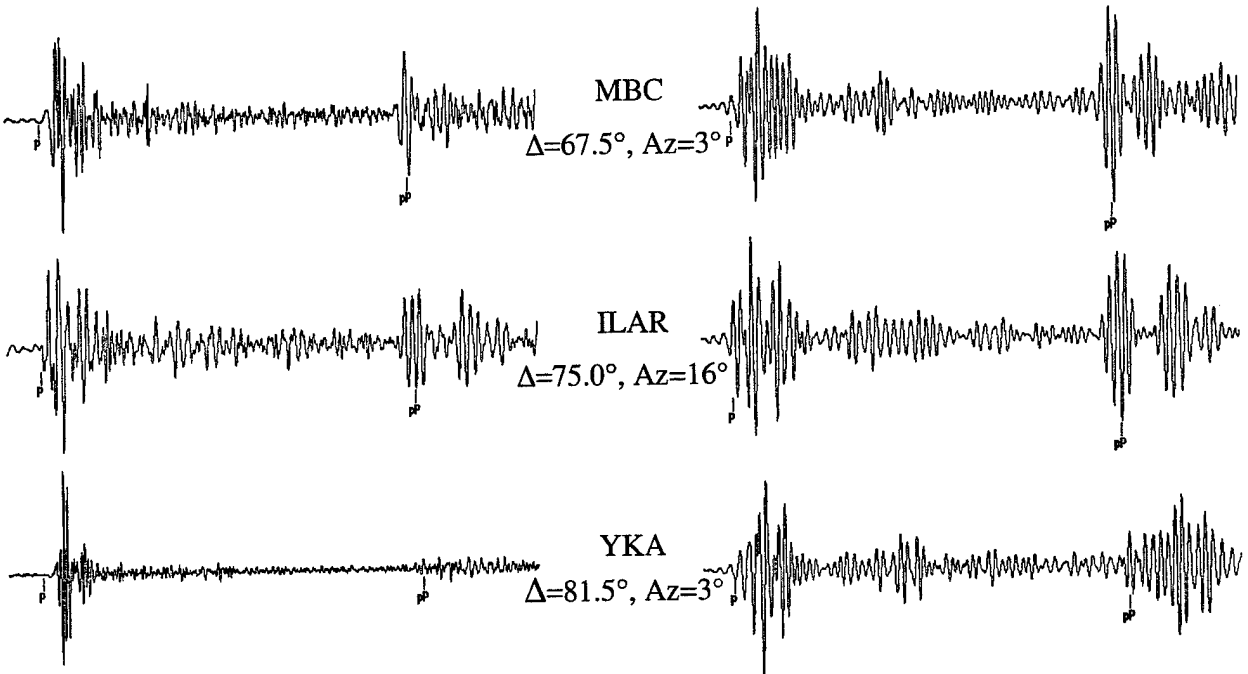

Figure 2-3. Comparison of broadband (left, 0.6 – 4.5 Hz) and lowpass filtered (right, 0.8 – 1.5 Hz) recordings of the southern Hindu Kush event of 1997/01/10 (h = 207 km) at the three nearby North American Stations MBC, ILAR and YKA.

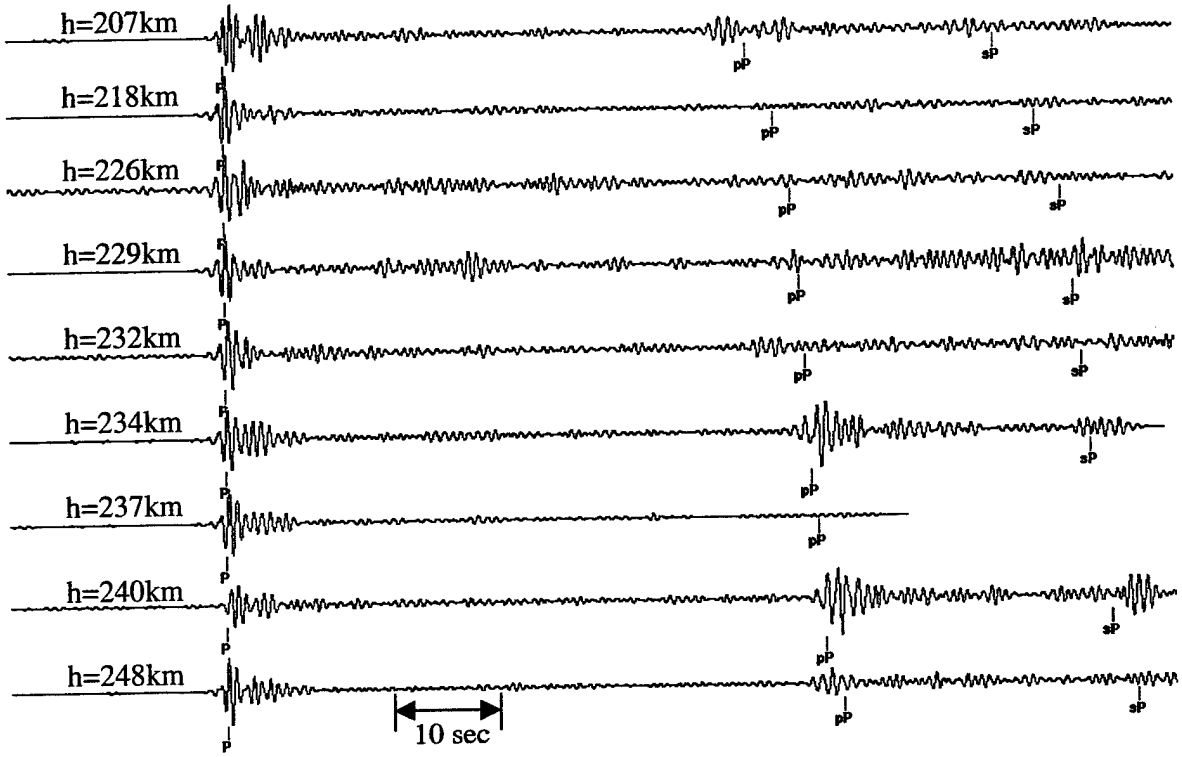

Figure 2-4. Comparison of station MBC (Δ=70°) bandpass filtered (1-2 Hz) recordings of selected Hindu Kush earthquakes with REB depths in the range 200 < h < 250 km.

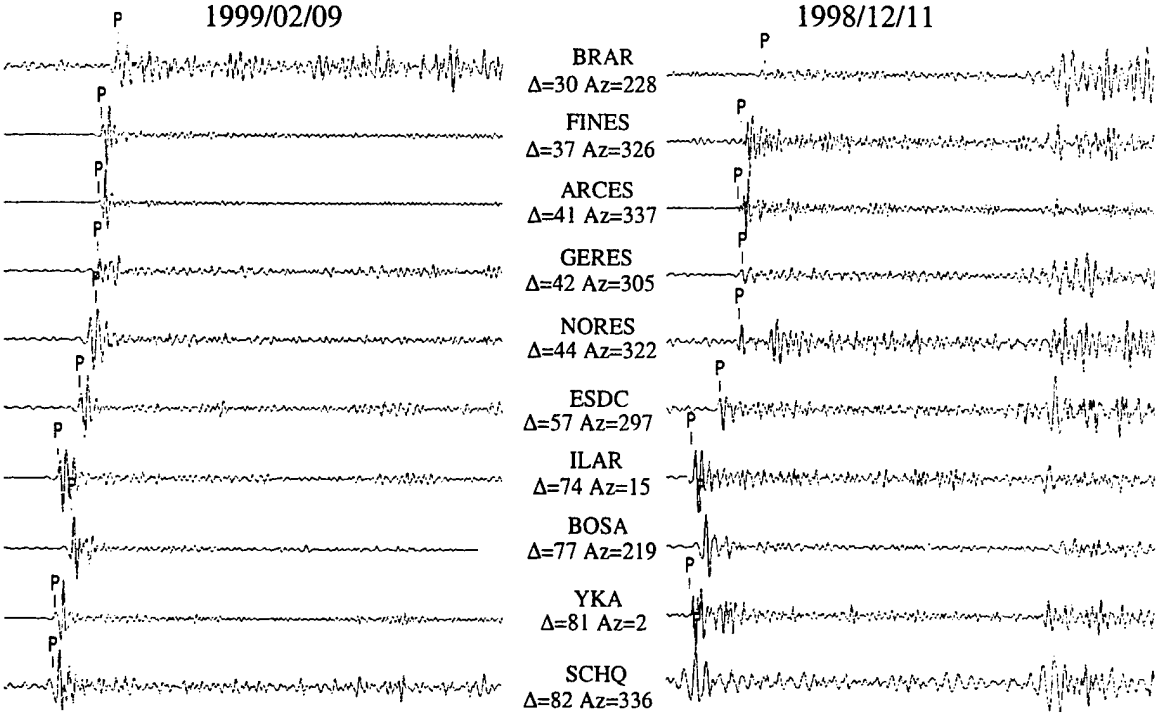

Figure 2-5. Comparison of recordings at common teleseismic stations from two nearby Hindu Kush events of comparable magnitude and depth.

and 228 km). It can be seen that for one of these earthquakes (1998/12/11, right) clear depth phases are evident at virtually every station; whereas for the other (1999/02/09, left) no depth phases are evident, despite the fact that these stations sample an azimuth window extending over nearly 180 degrees. Again, this type of variability makes it difficult to correlate arrivals between events, even in narrowly confined source regions.

A third complicating factor is the occasional occurrence of anomalous arrivals which are not predicted by the global travel time tables. Such "mystery phases" can have significant amplitudes and could be easily misidentified as depth phases in some cases. One interesting example of such a mystery phase is shown in

Figure 2-6 where recordings at station ESDC in Spain from a number of nearby Hindu Kush earthquakes are displayed in order of increasing focal depth between 190 and 243 km. Note the strong anomalous P arrival (P?) in the interval between P and pP which is only observed over a limited range of focal depth. In the absence of other information, it would be difficult for the analyst to resist identifying this arrival as a candidate depth phase, particularly in those cases where its amplitude is as large or larger than that of the true later arriving pP phase. Further investigation has revealed that this arrival is only observed from earthquakes in a very confined focal region. Other anomalous P phases have been observed from events in a variety of different source regions (eg. Kind and Seidl, 1982), which indicates that great care must be taken to conclusively validate candidate depth phase readings before they can be used to conclude with high confidence that an event is too deep to be an explosion.

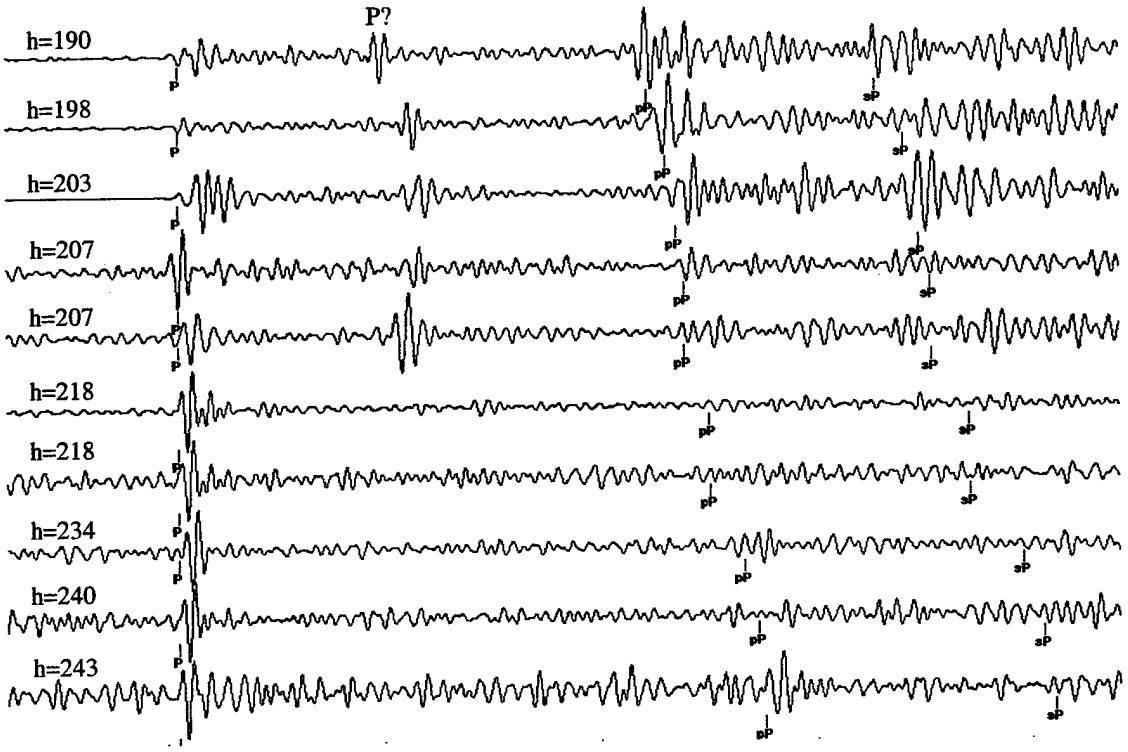

Figure 2-6. Comparison of station ESDC (Sonseca, Spain) recordings of selected Hindu Kush earthquakes with REB depths in the range 200 < h < 250 km.

2.2 APPLICATION OF NETWORK BEAMFORMING TO THE AUTOMATIC IDENTIFICATION OF CANDIDATE DEPTH PHASES.

In an attempt to overcome the various difficulties in single station depth phase identification illustrated in the preceding section, we have been investigating (Murphy et al, 2000) the potential utility of an automated network stacking algorithm which employs signal analysis procedures similar to those originally proposed by Israelsson (1994) and more recently applied to a sample of Canadian data by Woodgold (1999). The general problem is represented in simplified form in Figure 2-7 which shows synthetic pP and sP arrivals plotted at their predicted delay times with respect to P for a hypothetical Hindu Kush earthquake with a depth of 150 km. For simplicity, the arrivals are represented here by unit amplitude boxcar functions with constant widths of ±1 second for pP and ±1.5 second for sP. The trace at the bottom of this figure shows the direct sum of these individual synthetic traces, and it can be seen that the result is significantly degraded because the moveouts of the pP and sP pulses with respect to P as a function of epicentral distance have not been taken into account. Israelsson (1994) proposed to solve this problem by mapping the individual post-P arrivals observed at each station from functions of delay time with respect to P to functions of source depth using the pP-P or sP-P delay times predicted by the IASPEI 91 travel time tables for the individual station distances. This one to one mapping is illustrated in Figure 2-8 which shows the predicted pP moveout with respect to P as a function of source depth for two different epicentral distances. Using such predicted moveout curves, the observed delay times of all post-P arrivals with respect to P can be translated into equivalent focal depths under the hypothesis that they are pP or sP arrivals. Those arrivals which are consistent with such hypotheses should then add coherently and show up as pronounced peaks on the stacked network depth function. Figure 2-9 shows the result of applying this transformation to the

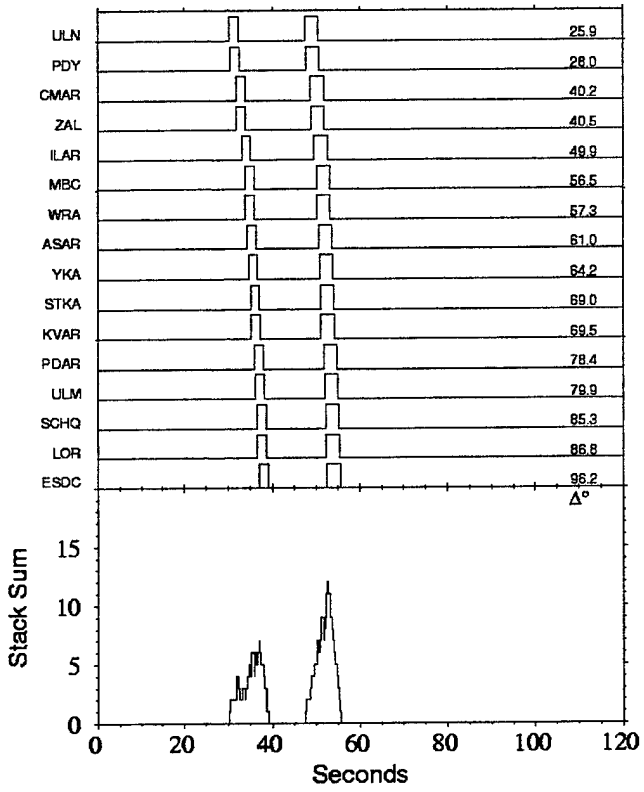

Figure 2-7. Synthetic pP and sP arrivals plotted at their predicted delay times with respect to P for a hypothetical Hindu Kush earthquake with a depth of 150 km. The bottom trace shows the direct sum of these individual synthetic arrivals.

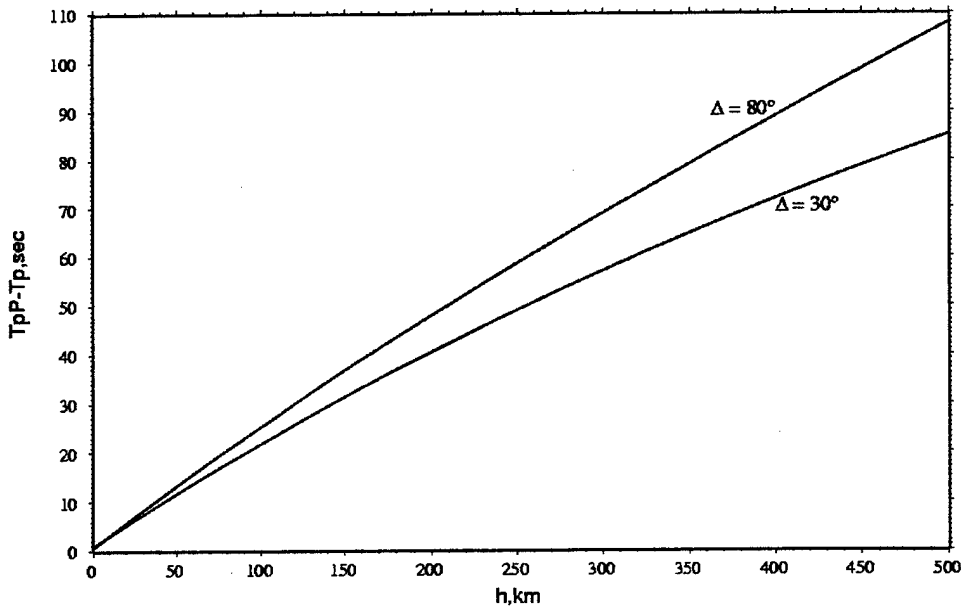

Figure 2-8. pP-P moveout times as a function of focal depth at fixed epicentral distances of 30 and 80 degrees.

synthetic arrivals of Figure 2-7 under the pP hypothesis. It can be seen that the network stack of these transformed synthetic traces produces a much sharper and larger amplitude peak than that obtained from the uncorrected direct sum shown in Figure 2-7.

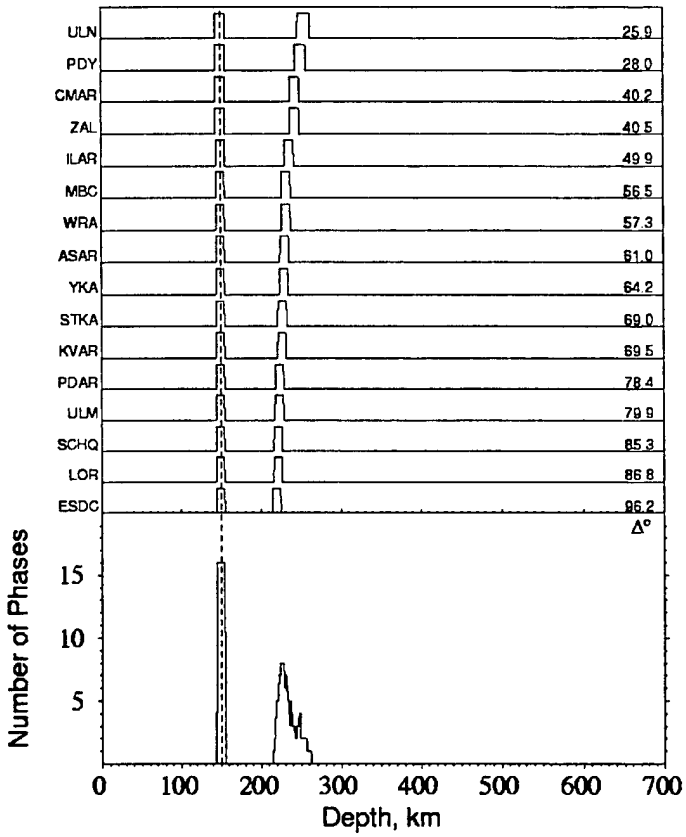

Figure 2-9. Network detection stack of pP as a function of candidate source depth corresponding to the previous synthetic example.

As was indicated by the examples shown in the previous section, one of the difficulties associated with the application of the above algorithm directly to the recorded short-period seismic data is that the depth phase waveforms and dominant frequencies for a given event can show substantial variability across a global network due to both focal mechanism and propagation path effects, which would

significantly degrade the effective gain of any direct network stacking procedure. Consequently, Israelsson (1994) and Woodgold (1999) formulated special purpose signal processing algorithms and station selection criteria in attempts to compensate for this lack of signal coherence between stations. In Murphy et al (2000) an alternate approach was adopted which is based on the automatic detection data produced by the detection processing employed at both the U.S. NDC and the IDC. In this approach, the observed post-P detection times in the detection file for a given event are used, together with their estimated uncertainties (currently taken to be ±1 second for pP and ±1.5 seconds for sP), to define unit amplitude boxcar functions centered on the automatic detection time; and these boxcars as functions of time are then mapped into equivalent boxcars as a function of source depth using predicted IASPEI 91 moveout curves such as those shown in Figure 2-8. It is these simplified functions of depth which are then stacked over the network of observing stations to identify candidate depth phases which are consistent with either the pP or sP hypothesis. An advantage of this approach is that not only is it fully automatic, but it only includes signals which have triggered one of the detectors, which should help to minimize the inclusion of questionable arrivals in the analysis. Figure 2-10 shows an example of the application of this algorithm to the automatic post-P detection times for a Hindu Kush earthquake on 1998/02/14. It can be seen that the network detection stack in this case shows a pronounced peak at a depth corresponding to the published REB depth for this event, indicating the presence of a good candidate pP phase which should be further reviewed by the analyst.

In Murphy et al (2000) the depth phase stacking algorithm described above was first applied to the automatic detection data from over 150 selected REB events

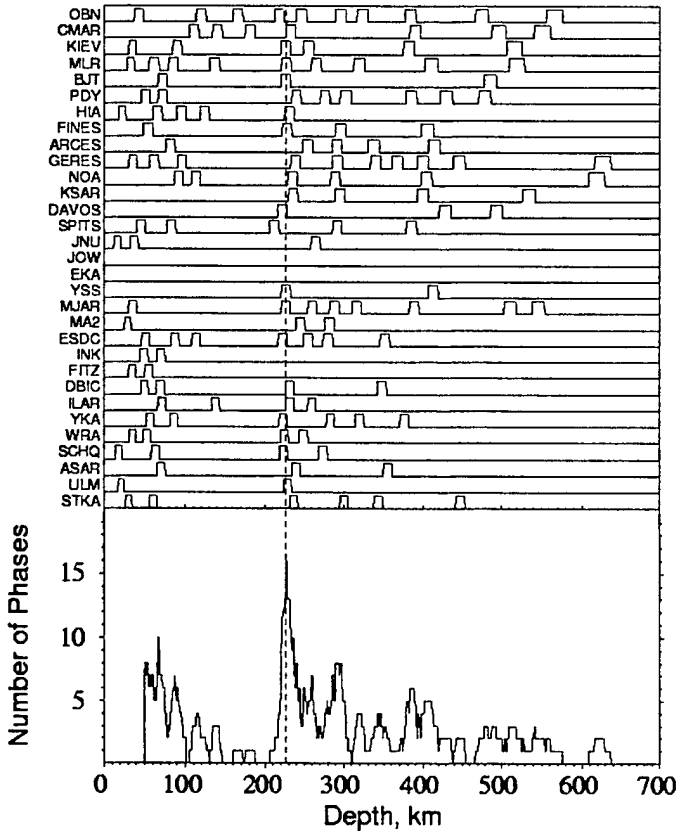

Figure 2-10. Network detection stack of pP for the Hindu Kush earthquake of 1998/02/14, m_b = 5.03. The dashed vertical line coincides with the REB depth estimate of 226 km.

located in the Hindu Kush, Lop Nor, Hokkaido and central Honshu regions identified on the map of Figure 2-11. Selected examples are shown in Figures 2-12 through 2-15. It can be seen that in all these examples there are prominent peaks on the network detection stacks which are either at or close to the corresponding REB depth estimates. In some cases, the REB depths do show some measureable offset with respect to the maxima of the corresponding network detection stacks. This reflects the fact that no depth phase data were used in determining the REB hypocentral solutions for these events and suggests that more accurate depths might have been determined for these events if the candidate depth phases

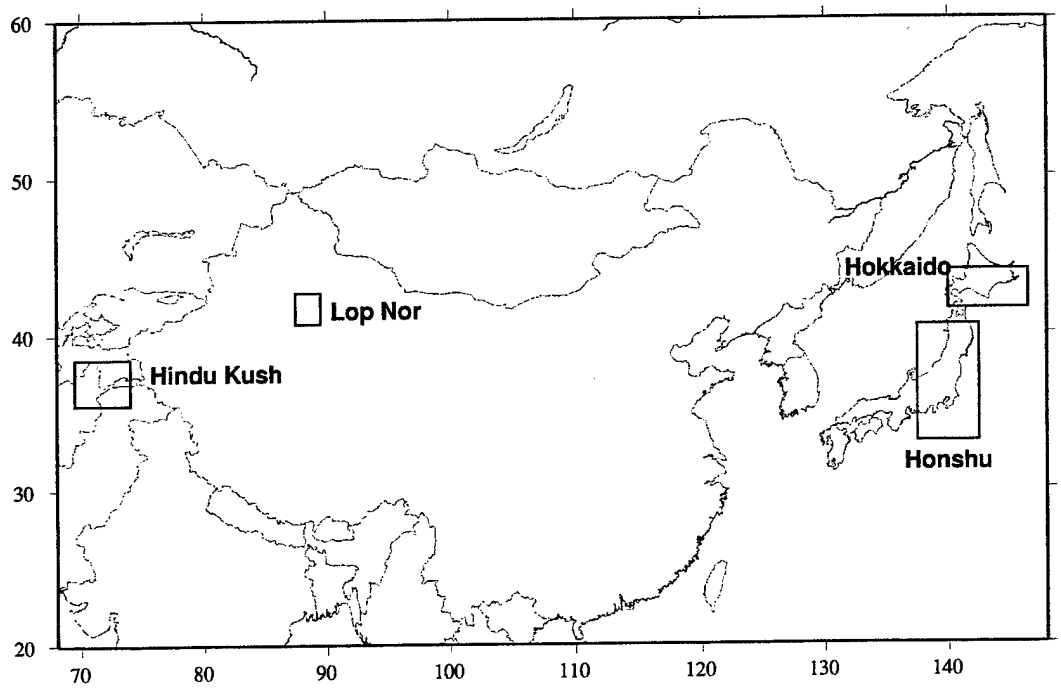

Figure 2-11. Map locations of the events used in the evaluation of the depth phase stacking algorithm.

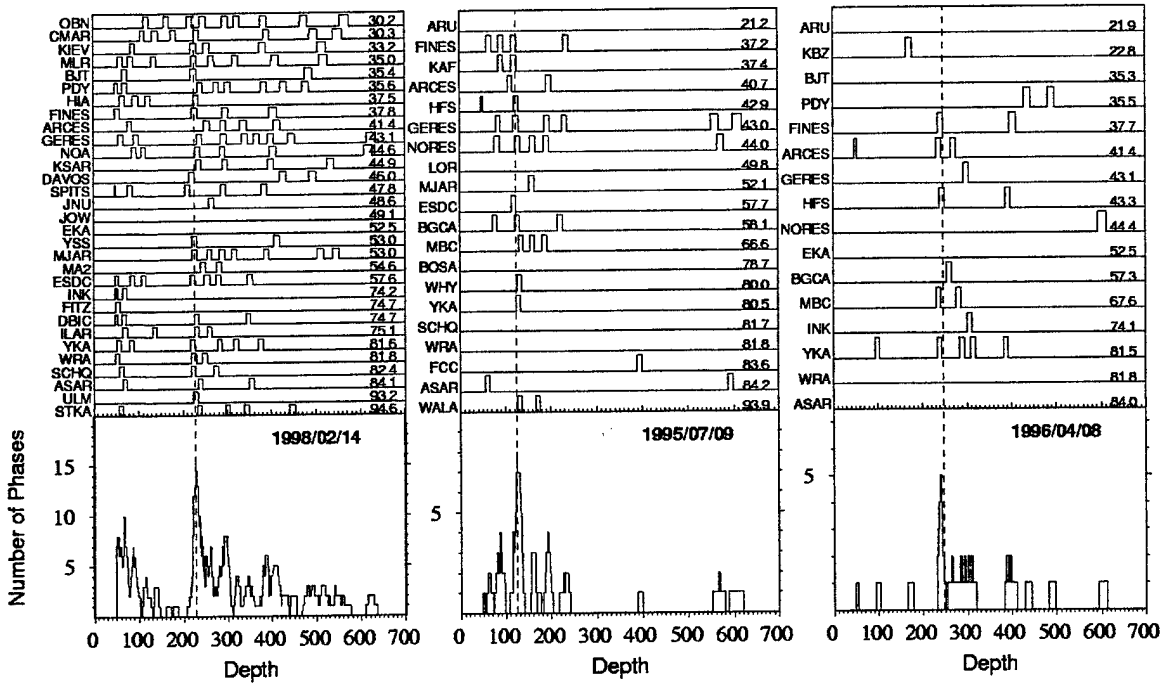

Figure 2-12. Network detection stacks of pP for the Hindu Kush earthquakes of 1998/02/14 (m_b = 5.03), 1995/07/09 (m_b = 4.40) and 1996/04/08 (m_b = 4.04).

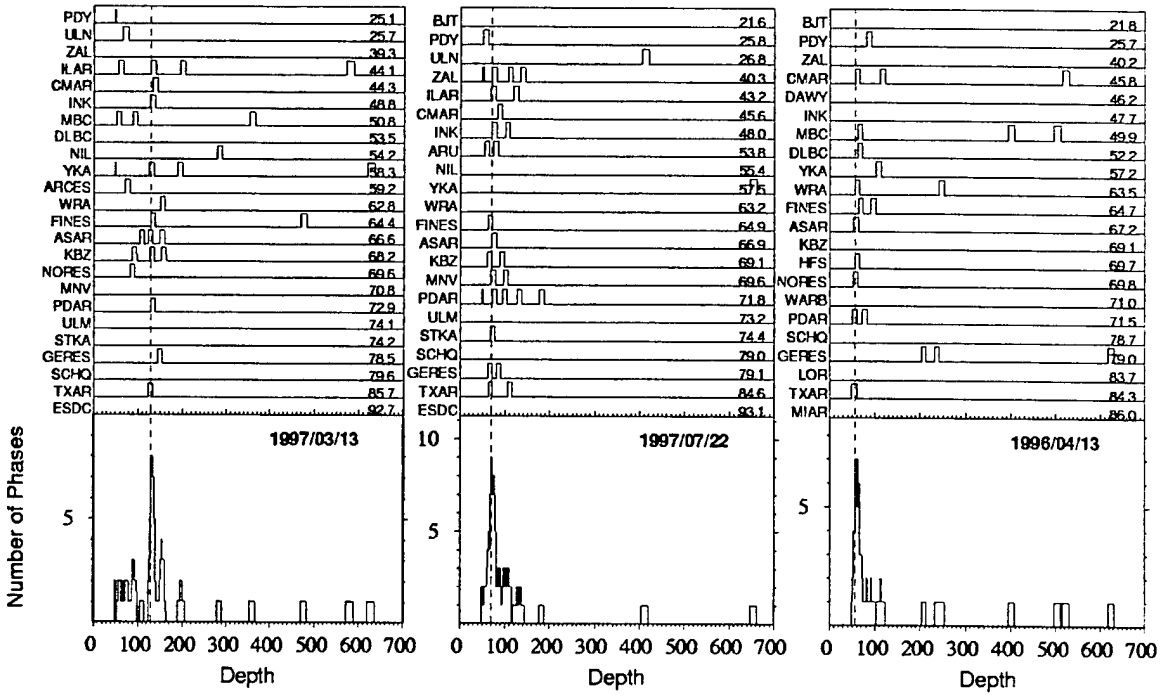

Figure 2-13. Network detection stacks of pP for the Hokkaido earthquakes of 1997/03/13 (m_b = 4.34), 1997/07/22 (m_b = 3.97) and 1996/04/13 (m_b = 3.82).

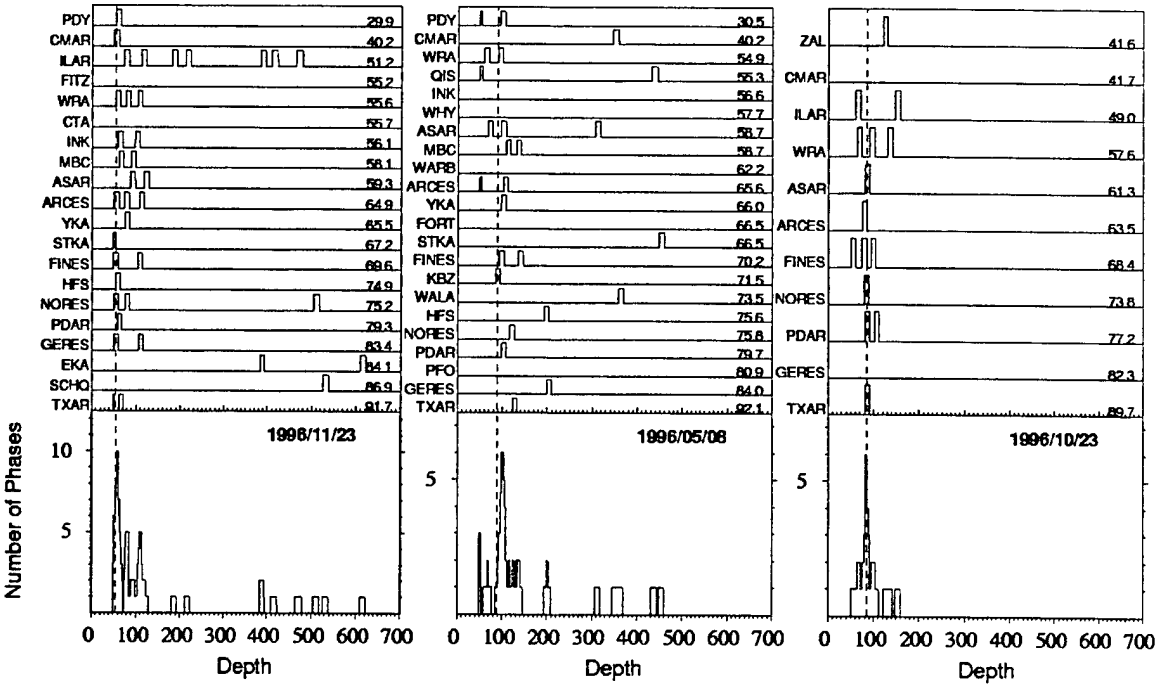

Figure 2-14. Network detection stacks of pP for the Central Honshu earthquakes of 1996/11/23 (m_b = 4.32), 1996/05/08 (m_b = 3.86) and 1996/10/23 (m_b = 3.79).

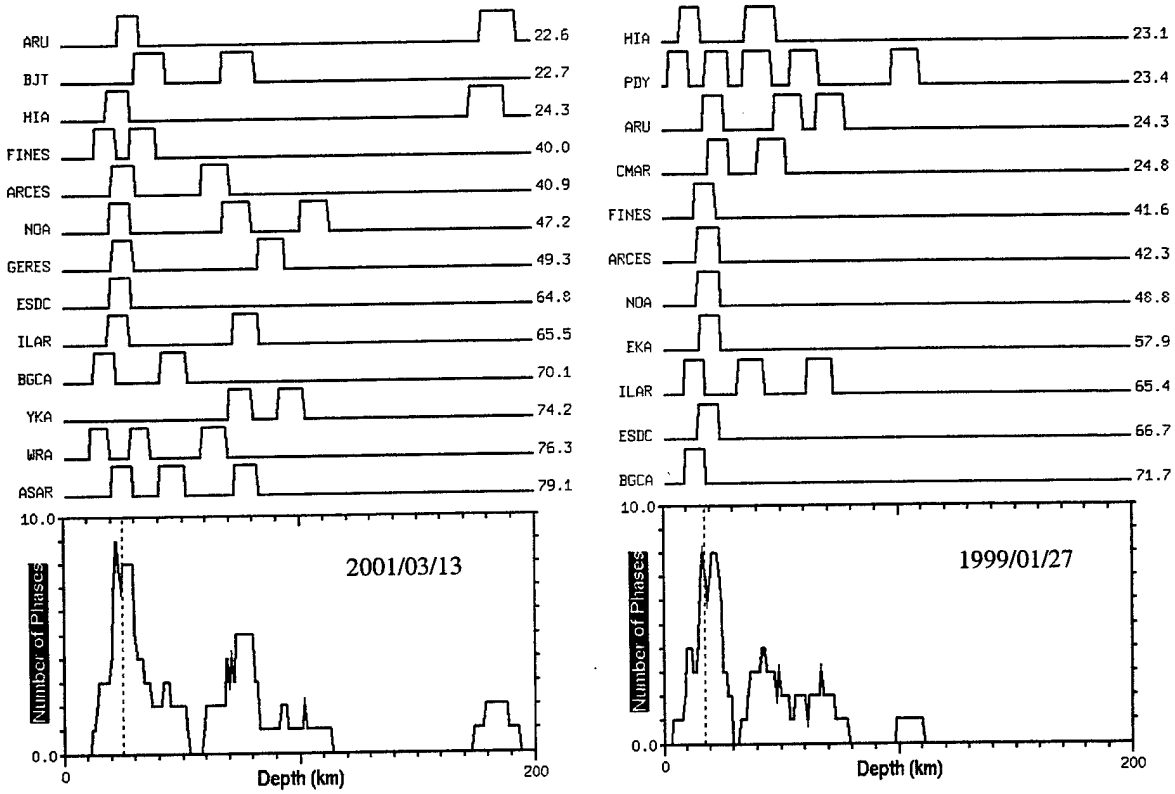

Figure 2-15. Network detection stacks of pP for the Lop Nor earthquakes of 2001/03/13 (m_b = 4.11) and 1999/01/27 (m_b = 4.01).

identified by the network stacking algorithm could have been validated and included in the hypocentral solutions. The results shown in Figures 2-12 through 2-15, along with other results we obtained (Murphy et al, 2000), document the fact that the proposed algorithm is applicable to events having m_b values as low as about 4.0 in the Hindu Kush region and about 3.75 in both the Hokkaido and central Honshu regions of Japan, with corresponding minimum depths of about 75 km and 55 km, respectively. Comparable results were obtained for over 70 % of

the events analyzed, which suggests this fully automatic algorithm could provide a powerful tool for directing an analyst to candidate depth phases which could be used in the event location process.

2.3 INTEGRATION INTO THE ANALYST REVIEW STATION

The Research and Development Support System (RDSS) developed by the Army Space and Missile Defense Center (SMDC) was established to improve nuclear explosion monitoring capability by supporting the R+D community with a broad range of activities and resources (Woodward and North, 2002). RDSS activities include providing environments for testing and evaluating promising research results at a range of scales. In order to make our depth phase stacking procedure available for large-scale testing and further evaluation the algorithm described above has been formally integrated into the RDSS Analyst Review Station (ARS) software which is employed at both the U.S. NDC and the IDC. This milestone now gives us the capability to evaluate our algorithm using the full-processing environment of the representative nuclear monitoring systems as well as historical data archives. During the interactive processing of an event, the analyst is able to initiate an automatic process from the ARS that causes all of the post-P detection times for the current event of interest to be recovered from the automatic detection files and passed to the depth phase stacking module, where they are converted into their corresponding depth traces, stacked, and presented back to the analyst in an interactive X-Window display. This interface to the depth-stacking algorithm in ARS is illustrated in Figure 2-16 and Figure 2-17, where we first show an example of the pP network detection stack for a Lop Nor region earthquake on 1999/01/27, followed by a summary of the pP, sP, and pP + sP stacks for this event. Note that the sum of the pP and sP stacks shows a pronounced candidate depth phase peak near the published, shallow REB depth of about 18 km for this earthquake. This

example is evidence that, at least in some cases, this depth stacking procedure can be applied to crustal events with depths shallower than 50 km. At this point in the ARS implementation of the procedure, by clicking on this or any other candidate depth-phase peak with the mouse, the analyst initiates a process by which the associated waveforms are brought up in the standard ARS display with the data time aligned on the predicted pP times corresponding to the selected trial depth. After this, the data can then be further processed by the analyst using the bandpass filter routine or any of the other signal processing algorithms available in the ARS. An ARS display for this Lop Nor earthquake is shown for selected stations in Figure 2-18, where it can be seen that there are multiple candidate pP and sP arrivals at the arrival times predicted for that selected trial depth. Moreover, in this case the variation of the pP/P amplitude ratios over wide ranges in distance and azimuth permit the analyst to identify pP and sP arrivals with high confidence, thereby enabling this event to be confidently screened out as a natural earthquake. This implementation of the algorithm has been employed by ARS analysts in their review of the data recorded from a large number of explosions and shallow earthquakes near Lop Nor as part of the Advanced Concept Demonstration (ACD), which was focused on improving the capability for monitoring the Chinese nuclear test site at Lop Nor. As part of that demonstration a total of 205 events were thoroughly analyzed by trained analysts. The results of this large scale test indicates that the new algorithm should be considered for incorporation into routine seismic analysis procedures such as those employed at the U.S. NDC or the IDC.

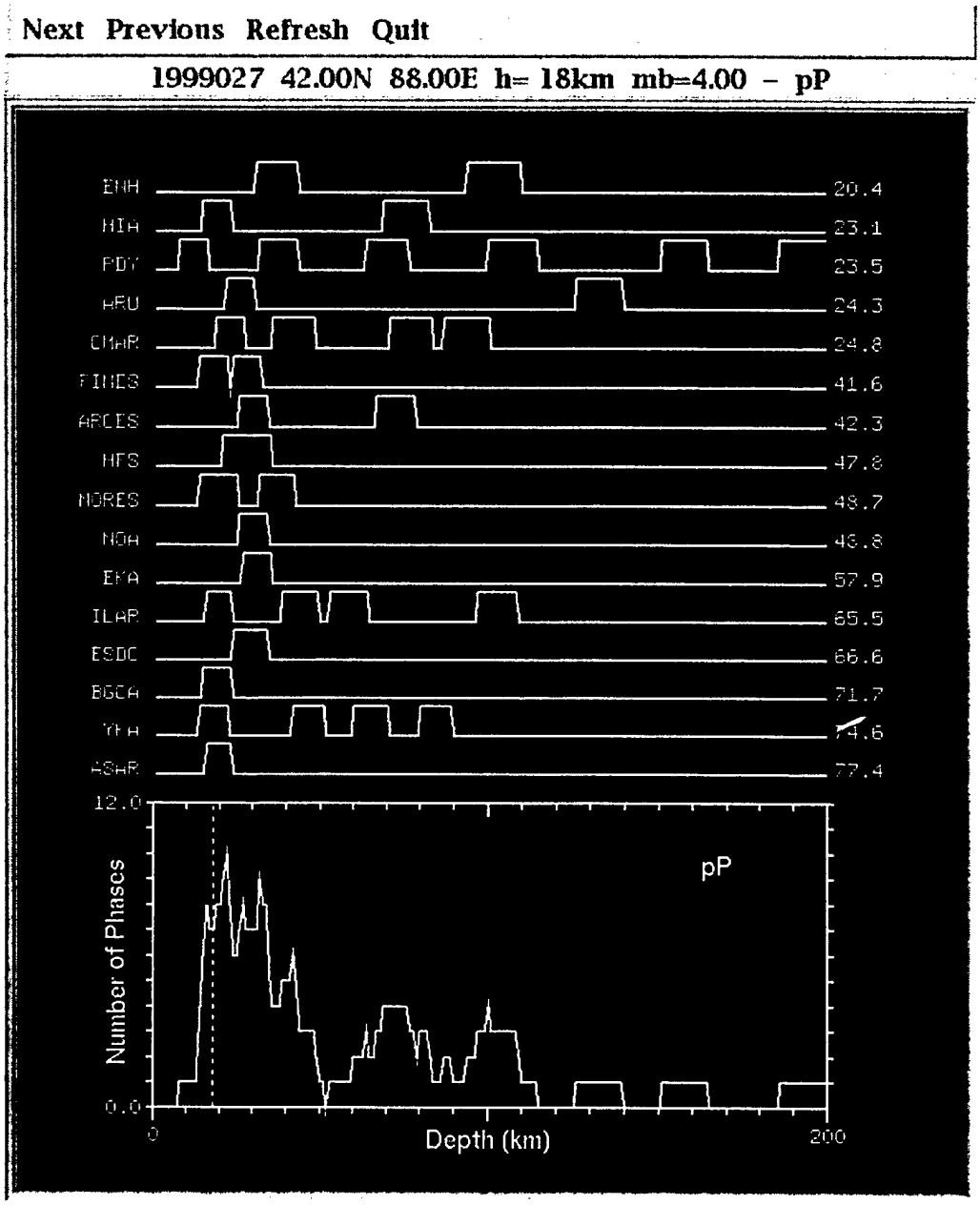

Figure 2-16. Network detection stack of pP for the Lop Nor region earthquake of 1999/01/27.

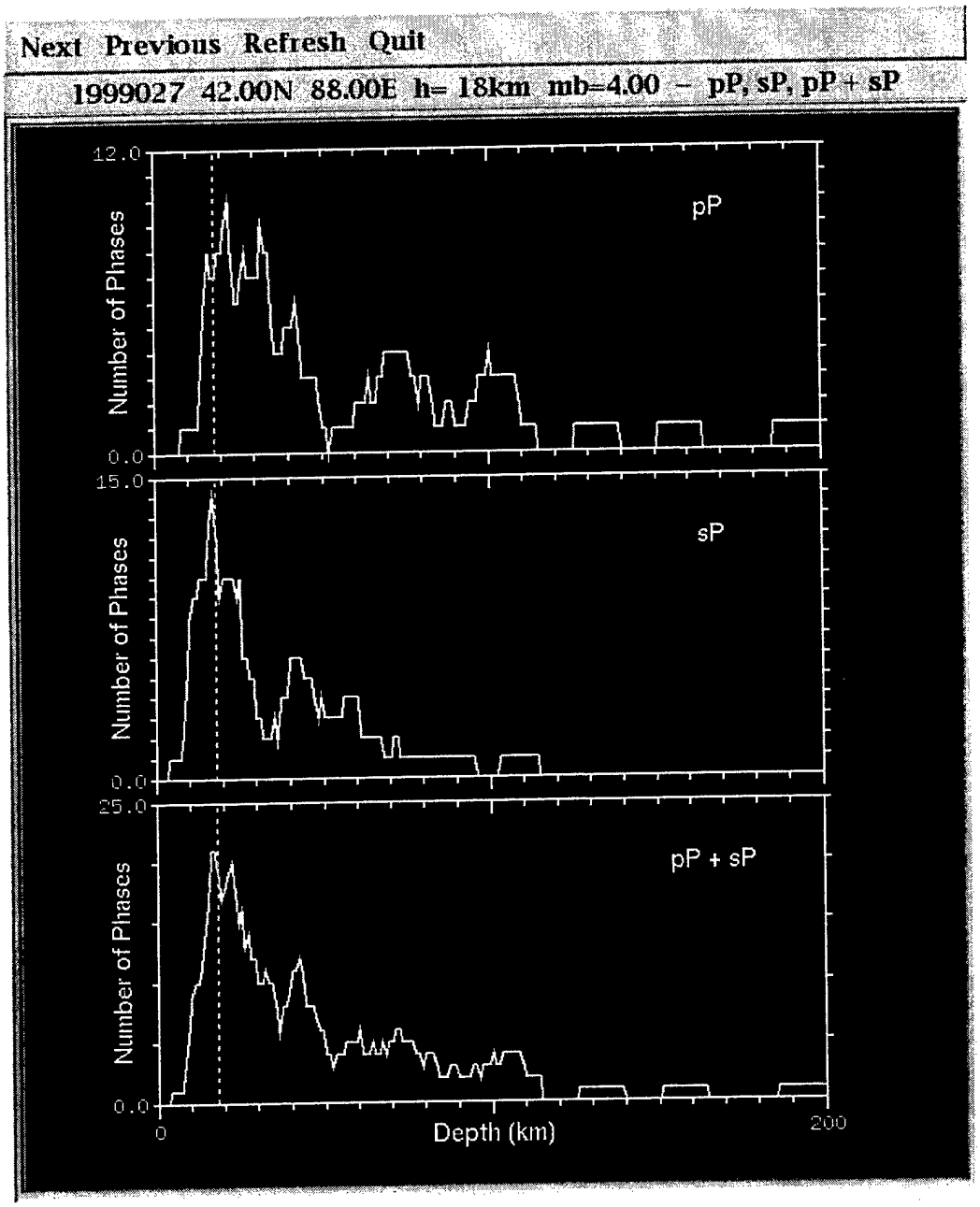

Figure 2-17. Network detection stacks of pP (top), sP (middle) and their sum (bottom) for the Lop Nor region earthquake of 1999/01/27.

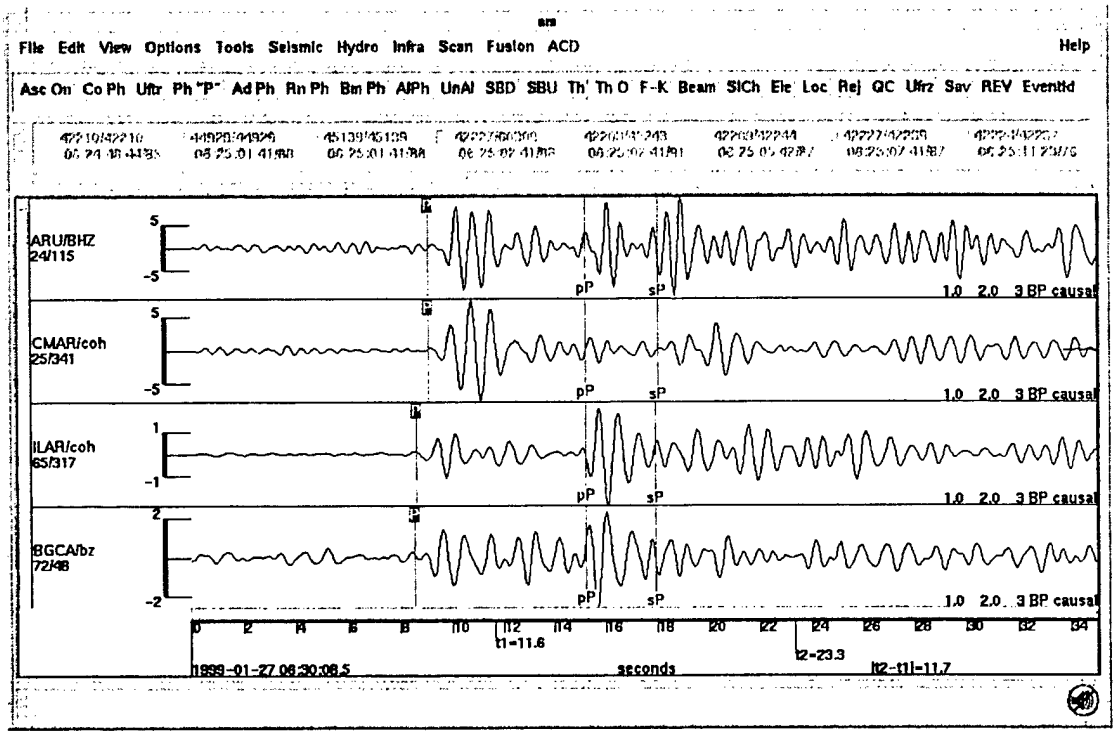

Figure 2-18. ARS display of bandpass filtered waveforms for the Lop Nor region earthquake of 1999/01/27, shown time aligned on the predicted pP arrival times corresponding to the selected candidate depth (i.e. 18 km) from Figure 2-17.

SECTION 3
VALIDATION OF CANDIDATE DEPTH PHASES

The network beamforming algorithm described above is proving to be a powerful tool for identifying candidate depth phases. However, the presence of a prominent peak on the network detection stack does not, by itself, constitute a positive identification which is confident enough to be used for purposes of event screening. Rather, it identifies possible depth phases which would have to be validated by further review and testing. That is, since the positive identification of a depth phase with a time delay of greater than about 3 seconds with respect to P conclusively identifies an event as being too deep to be an explosion, it is imperative that any such identification be made with a very high level of confidence. As a result, the development, implementation and testing of improved analyst tools and quantitative tests will play a key role in the completion of any new depth phase identification system. One such tool, the Pearce (1977,1980) focal mechanism algorithm, uses the observed relative amplitudes of pP and/or sP depth phases with respect to the P wave amplitude at each station in the network. The solution space of all double couple seismic sources is searched for possible solutions that are consistent with the relative amplitudes that are measured at each station. If no such solution can be found, then it must be concluded that either the candidate depth phases were misidentified or that the event was not a double couple (i.e. it must be considered as a potential explosion). Conversely, if a small number of consistent solutions are found which are compatible with the regional tectonics, then the confidence in the identification of the candidate depth phases would be greatly increased. Preliminary results (Murphy, et al, 2000) suggest that the Pearce focal mechanism algorithm may provide a valuable supplemental analyst tool for assessing candidate depth phases identified by the network stacking

procedure described in the previous section. Another tool that can be used in the characterization of network detection stack peaks is the F detector. The F detector (Blandford, 1974) operates on array station beam data and provides an output trace which is approximately equal to the time averaged power on the beam divided by N times the average variance of the individual channels and the beam, where N is the number of array stations. F can be approximated by:

$$F \approx (N-1)\frac{\sum_{t=1}^{M} u(t)^2}{\frac{1}{N}\sum_{t=1}^{M}\sum_{i=1}^{N} u_i(t)^2 - \sum_{t=1}^{M} u(t)^2} \qquad (3.1)$$

where $u(t)$ represents the beam output trace at time t from an N-element array of traces $u_i(t)$, and t = 1,...,M represents an averaging window of M samples. According to Blandford (1974), when a signal arrives with similar vector-slowness to the beam, F increases because, (1) the beam power in the numerator increases, and (2) the denominator is reduced to the residual noise. If a signal arrives from a significantly different vector-slowness to the beam, F is reduced as the denominator increases faster than the numerator. The potential value of the F detector in this context is that it provides a quantitative, statistical means of assessing the likelihood that a given arrival has the same vector slowness as the beam. Therefore, it provides a potential mechanism for evaluating whether detections at a station have characteristics that are consistent with what would be expected for pP and sP arrivals from the origin. This could provide a powerful means for eliminating false candidate peaks associated with source complexity or "mystery phases" like those identified in Section 2. We have implemented this algorithm in order to evaluate it's capabilities as a tool to assist in characterizing our depth phase stack peaks. For example, Figure 3-1 shows the results for an earthquake on July 9, 1997 located in the Honshu region of Japan and recorded at

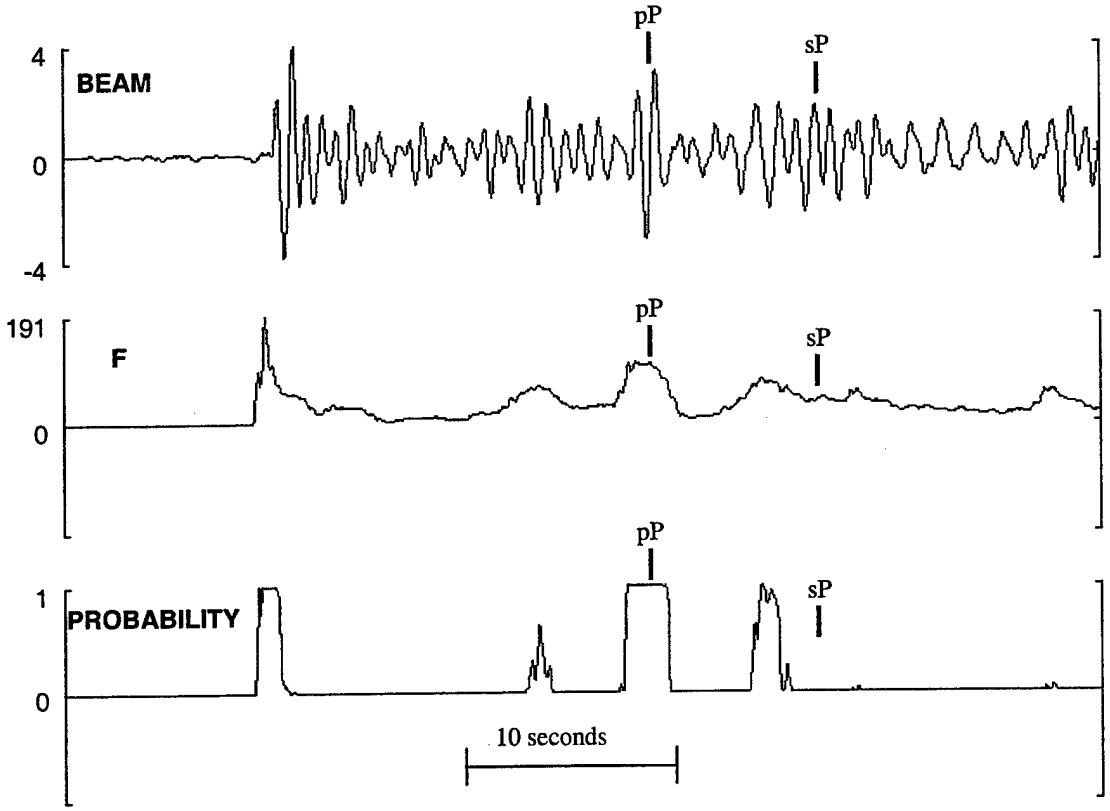

Figure 3-1. Best beam trace (top), F-trace (middle), and probability trace (bottom) at station YKA for the Central Honshu earthquake of 1997/07/09, mb = 3.94. The depth phase predictions are based on the REB depth of 71 km.

the YKA array in Canada. In the top of the figure is the beam trace steered to the location of the event and filtered between 0.5 and 3.0 Hz. The middle trace is the F detector trace, calculated using a 2 second moving window, and the bottom of the figure shows the F probability trace, which is derived from the F detector trace and indicates the probability that a phase is arriving at the same vector-slowness that the beam was steered to. Also marked on the traces are the predicted pP and sP arrivals for the estimated REB depth of 71 km for this event. It can be seen from the beam trace that there is energy arriving near the time of the predicted pP phase, energy that also appears on the F trace. The probability trace on the bottom shows that there is a high probability that this represents a phase arriving with the same

azimuth/slowness that the beam was steered to, giving us confidence that it might represent a true depth phase. The sP phase results are not as clear, however, with no distinct phase appearing on any of the traces at the expected arrival time. It might be that this phase is buried in the coda of another, unpredicted phase arriving a few seconds earlier than the expected time for sP. We have also applied this algorithm to the station YKA recordings of the shallow Lop Nor earthquake of 1999/01/27 discussed in Section 2. The results of this application are shown in Figure 3-2. Marked on the figure are the predicted pP and sP times for the REB assigned depth of 18 km, in agreement with the peak of our depth phase stack from Section 2 (cf. Figure 2-16). Again, we see evidence in these results that the

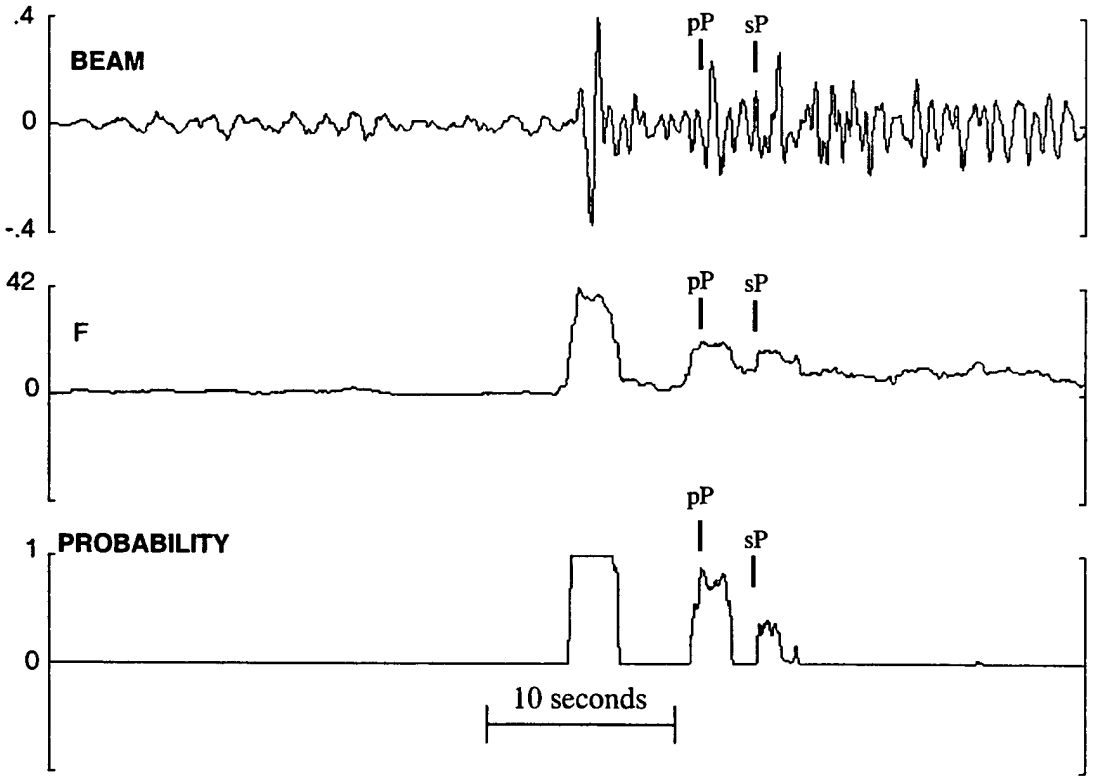

Figure 3-2. Beam trace (top), F-trace (middle), and probability trace (bottom) at station YKA for the Lop Nor earthquake of 1999/01/27, $m_b = 3.90$. The depth phase predictions are based on the REB depth of 18 km.

candidate depth phases are being generated by this source and as indicated by the probability trace we could say with some confidence that they correspond to the depth phases pP and sP. So it appears that this F detector algorithm might be useful in the characterization of peaks resulting from our network stacking procedure.

In order to validate candidate depth phases, we have developed a scheme for weighing our depth phase stacking results with the results of the F detector processing. In this procedure we start with the depth phase stacking results, an example of which is shown in Figure 3-3 for the Hokkaido earthquake of 1997/07/01. It can be seen from this figure that there are a number of prominent peaks on the network detection stack, suggesting a number of candidate depth phases which need to be further evaluated. From this display we then extract the detections for the array stations contributing to the peaks; these are shown as functions of candidate depth in Figure 3-4. Next, the F detector is run on the waveforms at each of the arrays to give us the detection probabilities as a function of depth, as shown in Figure 3-5. These probabilities are then used to weight the original detection traces and the depth stack is re-calculated from the weighted traces. These results are shown in Figure 3-6, where it can be seen that a number of the secondary stack peaks from Figure 3-3 have been suppressed, while the peak corresponding to the REB estimated depth has been retained. Thus, these results show that we are able to use the F detector output to provide a valuable supplemental analyst tool for assessing candidate depth phases identified by the network detection stacking procedure. Additional encouraging results are shown in Figure 3-7 for the central Honshu earthquake of 1997/07/09, where again the weighting procedure is successful at suppressing secondary peaks while retaining the main peak. Figure 3-8 shows additional results for the Hokkaido earthquake of

1997/03/13. These results are even more convincing with the only remaining peak being the one corresponding to the estimated REB depth.

In summary, these preliminary results indicate that the combined use of the network stacking algorithm with the F detector has excellent potential for greatly improving the confidence in depth phase identification.

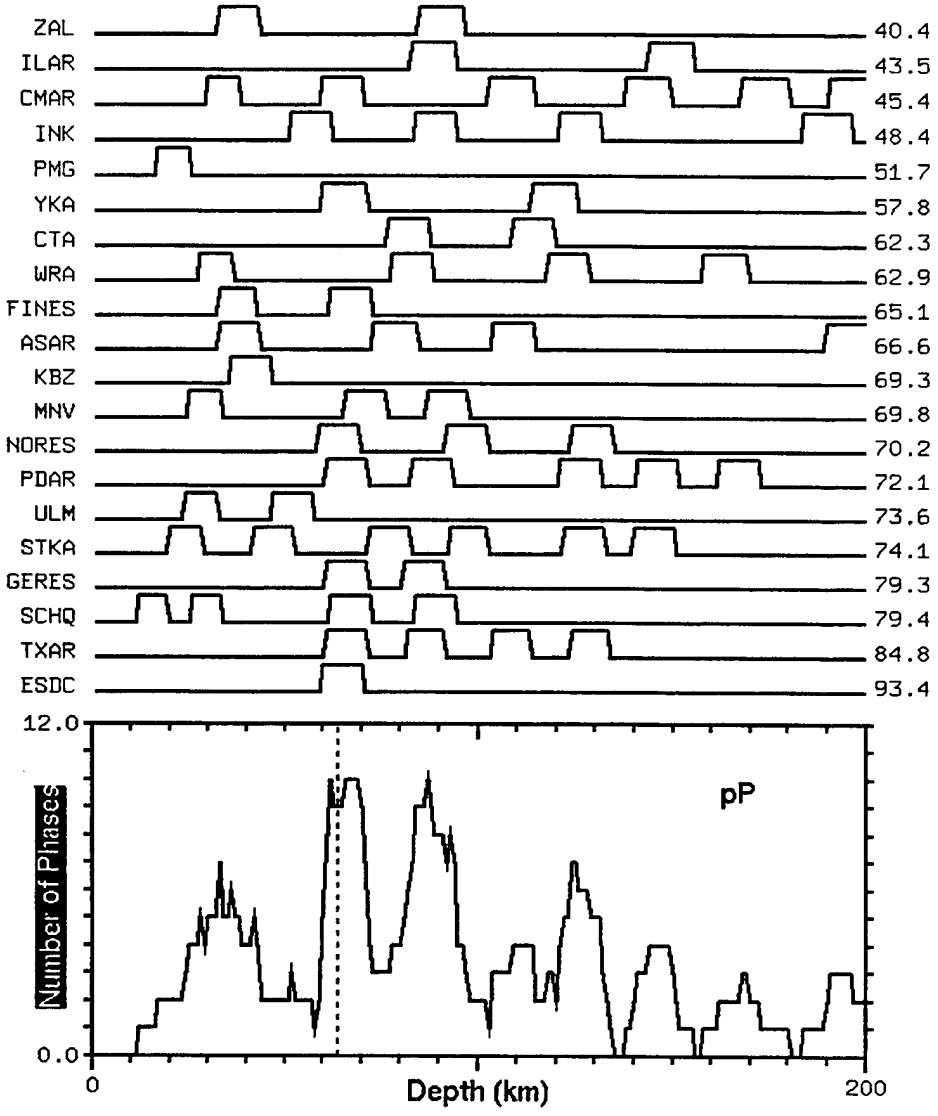

Figure 3-3. Network detection stack of pP for the Hokkaido earthquake of 1997/07/01. The dashed vertical line coincides with the REB depth estimate of 63 km.

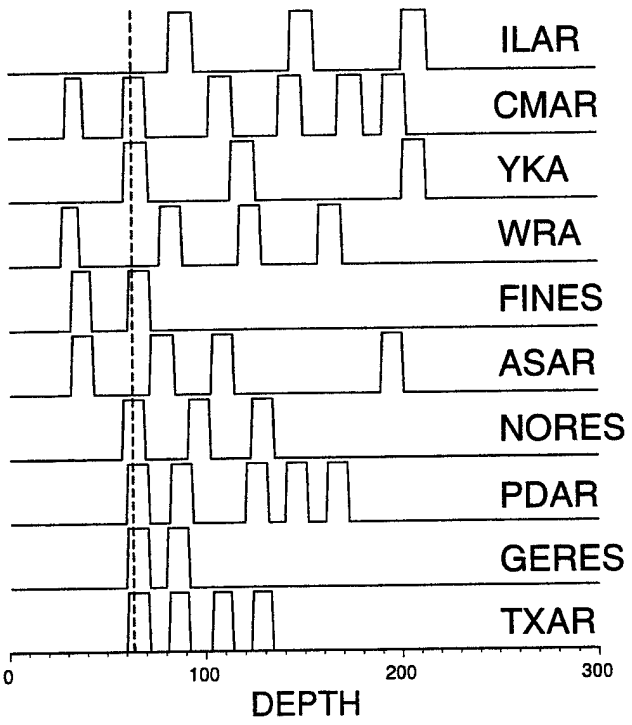

Figure 3-4. Depth traces for the array stations of Figure 3-3. The dashed vertical line coincides with the REB depth estimate of 63 km.

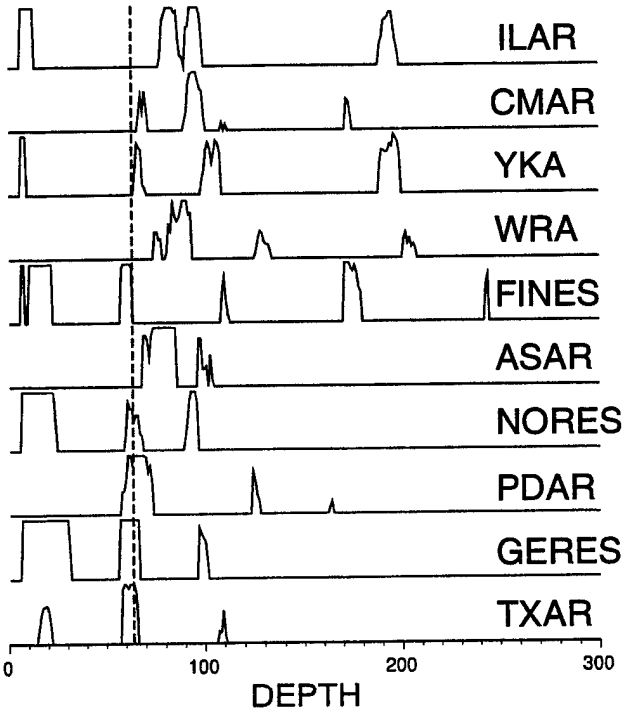

Figure 3-5. F probability traces for the array stations of Figure 3-3. The dashed vertical line coincides with the REB depth estimate of 63 km.

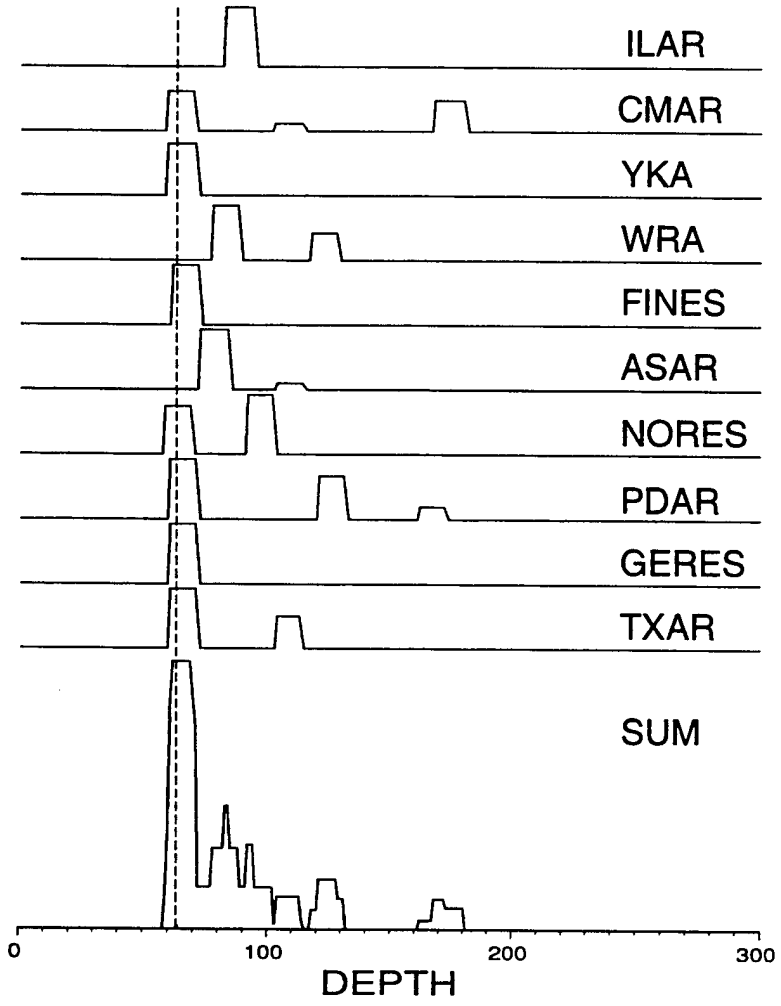

Figure 3-6. Weighted network detection stack of pP for the Hokkaido earthquake of 1997/07/01. The dashed vertical line coincides with the REB depth estimate of 63 km.

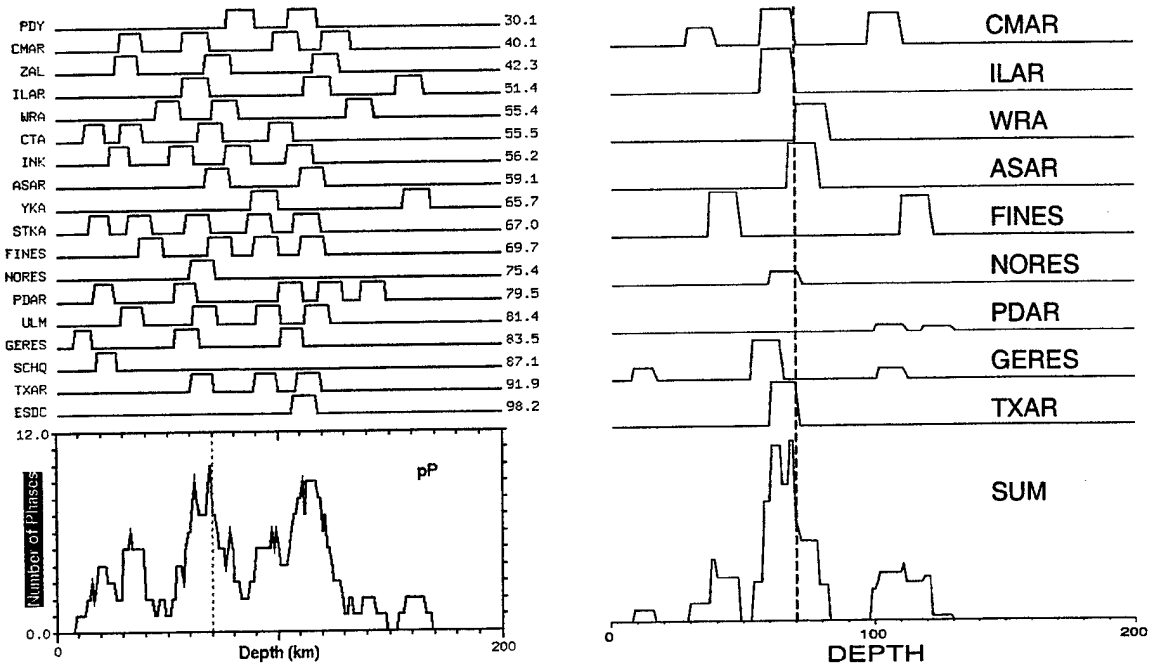

Figure 3-7. Comparison of original (left) and F detector weighted (right) network detection stacks of pP for the Honshu earthquake of 1997/07/09. The dashed vertical line coincides with the REB depth estimate of 70 km.

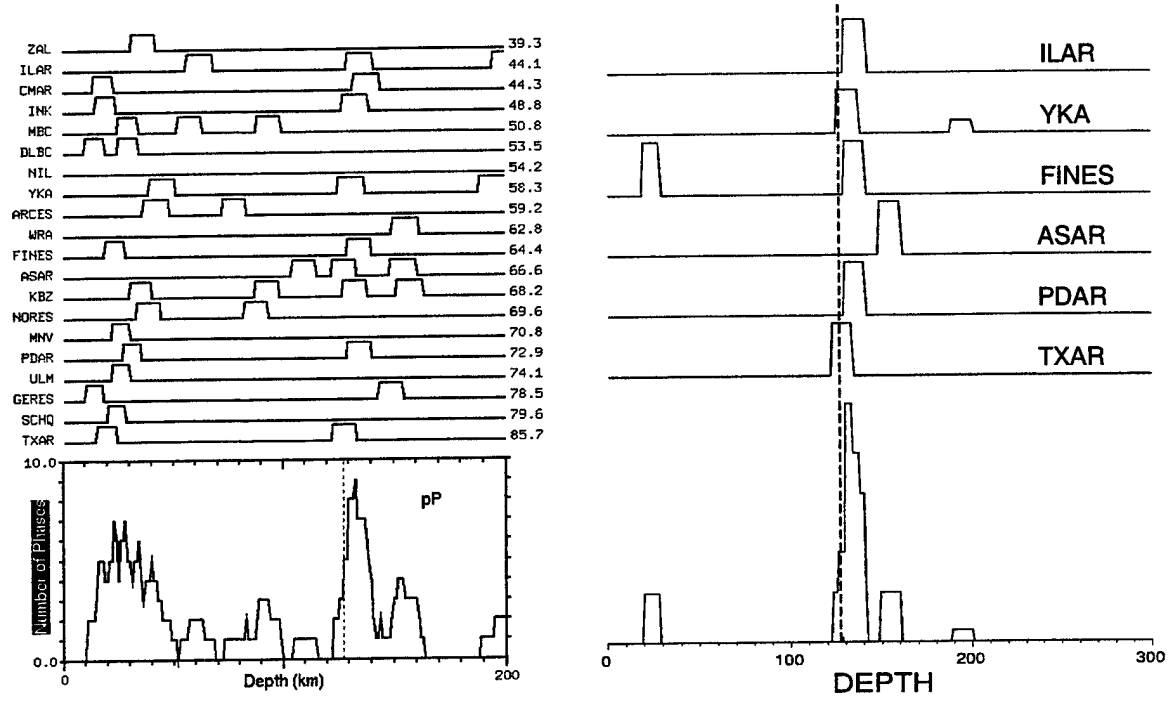

Figure 3-8. Comparison of original (left) and F detector weighted (right) network detection stacks of pP for the Hokkaido earthquake of 1997/03/13. The dashed vertical line coincides with the REB depth estimate of 128 km.

SECTION 4

FOCAL DEPTH ESTIMATION BASED ON REGIONAL S MINUS P TIMES

As was noted previously above, only 20% of the free depth solutions in the GSETT-3 database were based on depth phase observations. It follows that, even if depth phase identification can be significantly improved by employing new techniques such as the network beamforming procedures described in Section 2, there will still be many earthquakes for which focal depth can only be estimated through analyses of the observed P wave first arrival times. Therefore, it is appropriate to consider the various factors affecting the accuracy of such estimates. One obvious, fundamental limitation in depth resolution is associated with the magnitudes of the differences in the expected P wave first arrival times between events with different focal depths, relative to the errors in the arrival time readings. This issue is graphically illustrated in Figure 4-1, where the differences in P wave arrival times predicted by the IASPEI 91 tables between an event with a focal depth of h=0 and events with the same epicenter having focal depths of 100 and 200 km are displayed as functions of epicentral distance. Considering first the event with a depth of 100 km, it is interesting to note that for distances greater than about 25°, the differences in arrival times can be very closely approximated by a linear relation of the form $\Delta\tau = \Delta\tau_0 - \alpha\Delta$ where $\Delta\tau_0 \approx -9.9$ seconds and $\alpha \approx -0.035$ seconds/degree. Now consider the hypothetical situation where arrival time data are available from a 100 km deep event from a large network with stations well-distributed with respect to azimuth over the distance range $25° < \Delta < 90°$. Assuming these data contain no systematic errors, a hypocenter solution determined under the constraint h = 0 will give the correct epicenter with an

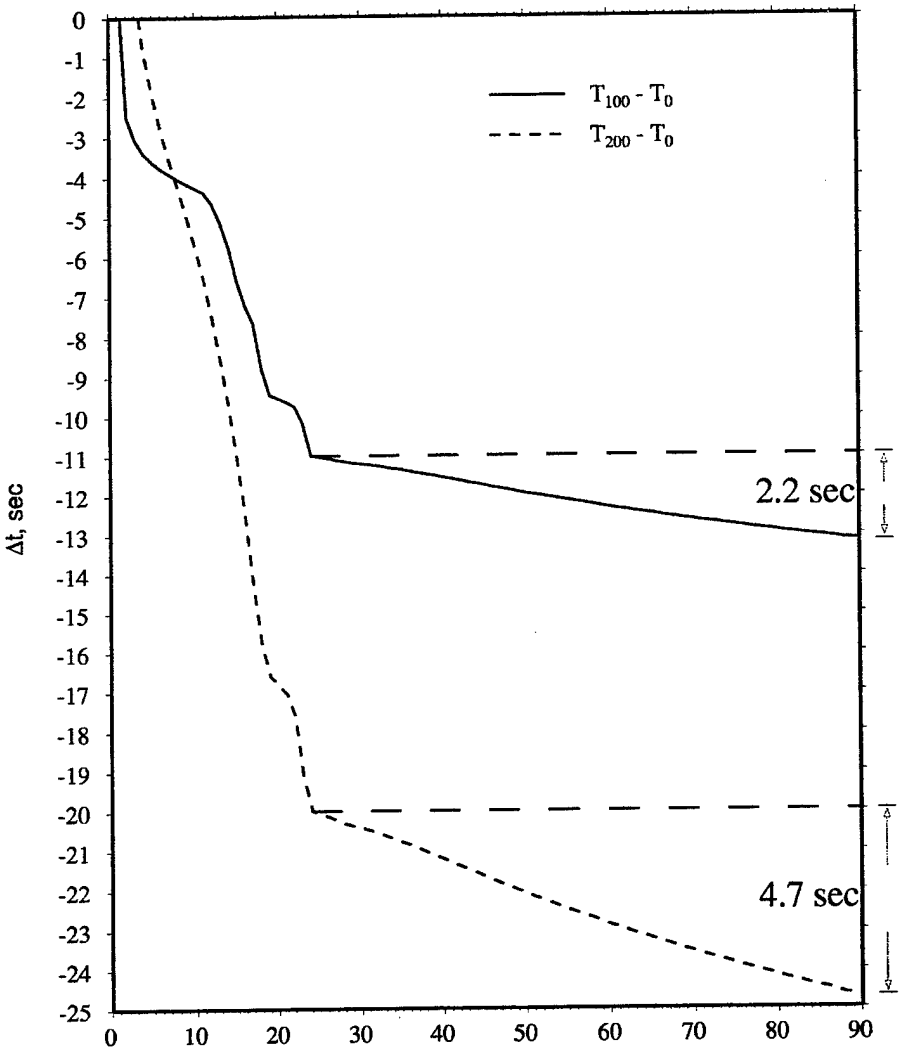

Figure 4-1. Differences in P wave arrival times as a function of distance predicted by the IASPEI 91 tables between an event with a focal depth of h = 0 and events at the same epicenter having focal depths of 100 and 200 km.

associated origin time which is about 12 seconds earlier than the true origin time. This is the often referred to trade off between focal depth and origin time. The travel time residuals with respect to this constrained solution would be uniformly distributed over the range extending from –1.0 to + 1.0 seconds, which is comparable to the expected error bounds on observed teleseismic P wave arrival time data. Thus, even with station-corrected data, teleseismic P wave first arrival

times for events with focal depths of up to 100 km or more can't be used to confidently conclude that such events are too deep to be explosions, even with an ideal network of stations located at distances of greater than 25°. Although the detailed nature of this trade-off between focal depth and origin time can be complex in practical applications to small events, an ability to independently constrain the event origin time can nonetheless be shown to lead to significantly improved focal depth estimates. More specifically, if S-P differential arrival time information is available from well-calibrated regional stations, it can be used to provide useful, independent estimates of the event origin time for use as constraints in the hypocenter location process. That is, if t_0 is the event origin time and t_P and t_S are the observed arrival times of P and S waves that have traveled essentially the same path to a station at distance Δ from the event, it follows that:

$$\begin{aligned} t_P &= t_0 + T_P(\Delta, h) \\ t_S &= t_0 + T_S(\Delta, h) \end{aligned} \qquad (4.1)$$

where h denotes the focal depth and T_P, T_S are the travel-time functions for P and S arrivals as a function of epicentral distance and focal depth. It follows that we can relate the origin time to the observed S-P time interval as

$$t_P - t_0 = \frac{1}{\left[\frac{T_S(\Delta,h)}{T_P(\Delta,h)} - 1\right]}(t_S - t_P) \qquad (4.2)$$

or

$$t_0 = t_P - \frac{1}{\left[\frac{T_S(\Delta,h)}{T_P(\Delta,h)} - 1\right]}(t_S - t_P) \qquad (4.3)$$

Now, if the travel paths for the observed P and S arrivals are the same and the ratio of compressional (α) to shear (β) wave velocity along these paths is constant, independent of Δ and h, then (3) can be simplified to

$$t_0 = t_P - \frac{1}{\left[\frac{\alpha}{\beta} - 1\right]}(t_S - t_P) \qquad (4.4)$$

which is the relation originally proposed by Wadati some 75 years ago in his studies of deep, Japanese earthquakes. It follows that if the average ratio α/β along paths to a selected regional station from events in a specified source region can be determined, then the event origin time can be estimated from observed P and S arrival times.

More formally, for a fixed event with m observations, the hypocentral uncertainty due to random picking errors is given by the 3 x 3 variance matrix of the hypocenter, which in turn is determined by the slowness vectors (at the hypocenter) for the m rays that were observed. The trade-off of location with origin time is accounted for by removing the mean of these slowness vectors prior to computing the variance matrix. If all the data are teleseismic P waves, the vertical components of all the slowness vectors are approximately the same and depth resolution will be poor. To increase depth information, it is necessary to add data for which the vertical components of the slowness vectors are significantly different from those of the teleseismic P data. One way to accomplish this is to add a regional S-P based origin time estimate, which is associated with a slowness vector of zero. That is, if the observed P and S arrival times at some regional station are represented by equations 4.1 above, then since tp-to is approximately a

linear function of t_S-t_P, it follows that T_S can be represented as a linear function of T_P

$$T_S(\Delta,h) = a + bT_P(\Delta,h) \tag{4.5}$$

where a,b are calibration constants. Then, given observations of t_O, t_S, we can solve for the origin time as

$$t_O = \frac{a + bt_P - t_S}{b-1} \tag{4.6}$$

Note that, as a consequence of the assumed linear relation between T_P and T_S, this origin time estimate is independent of any estimate of the hypocenter. We are currently developing a formal error model which will rigorously account for the effects of uncertainties in the calibration constants a and b on the corresponding uncertainty in the resulting focal depth estimate.

An illustration of the power of calibrated regional S-P data in constraining event focal depth can be seen in Figure 4-2, where we show a comparison of t_S - t_P variation as a function of focal depth predicted at a fixed near-regional distance of 5° by the IASPEI91 travel time tables with the corresponding predicted variation in P wave first arrival times at a nominal distance of 45°. For $20 \leq h \leq 100$ km, t_S- t_P is essentially independent of depth in the regional distance range $2° < \Delta < 10°$, while t_P at $\Delta = 45°$ decreases by more than 1 sec for every 10 km increase in h.

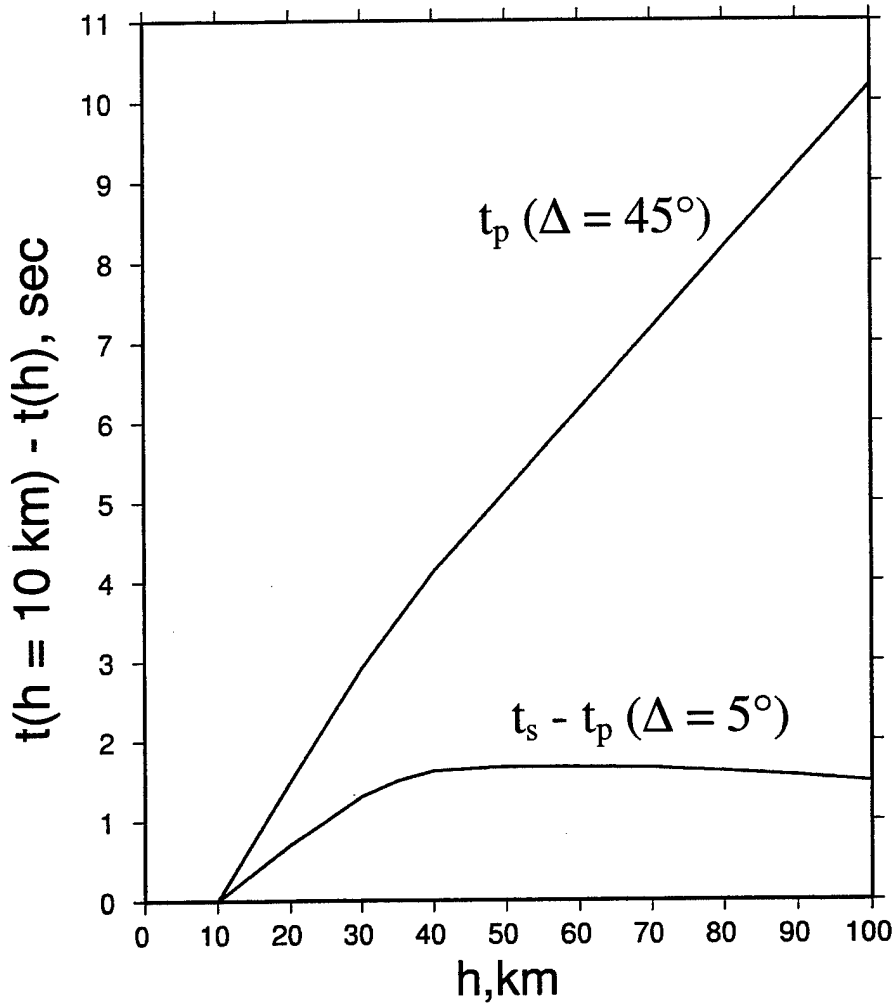

Figure 4-2. Comparison of t_s-t_p variation as a function of focal depth predicted at a fixed near-regional distance of 5° by the IASPEI91 travel time tables with the corresponding predicted variation in P wave first arrival times at a nominal distance of 45°.

Therefore, such regional data, if properly calibrated, provide very robust constraints on origin time and the associated depth estimate.

An application of this constrained origin time procedure is illustrated in Figure 4-3, where we show a comparison of differences in depths estimated from teleseismic P arrival times with respect to the "true" depth phase constrained values for 47 Honshu earthquakes in the depth range of 50 to 150 km, obtained with and without

origin time constraints. These results indicate that earthquakes with depths greater than about 30 km in this region can be shown to be too deep to be explosions at a very high level of confidence if S – P constrained origin times are available.

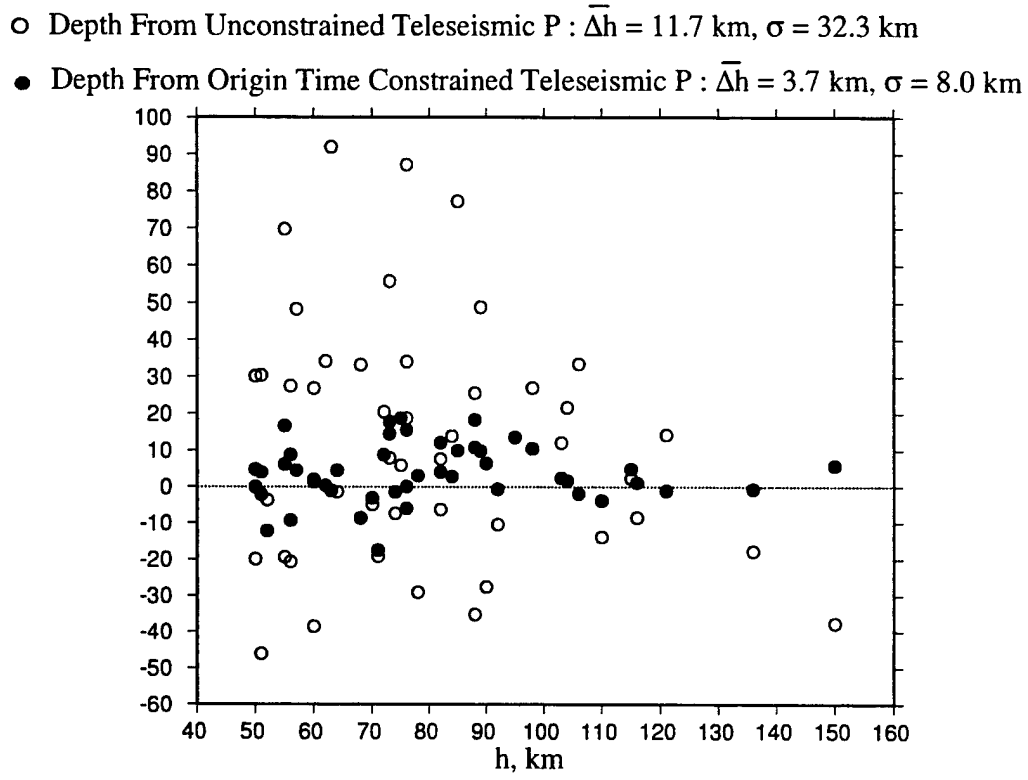

Figure 4-3. Comparison of differences in estimated depth with respect to the "true" depth phase constrained values for 47 Honshu earthquakes in the depth range of 50 to 150 km obtained with and without origin time constraints.

We have formulated a focal depth hypothesis test by comparing this S-P-based origin time estimate, t_0(S-P), with the corresponding teleseismic-based origin time, $\tilde{t}_0\,(h = 0\,\text{km})$, determined with the depth constrained to zero. Substantial differences in these two estimates provide evidence of significant focal depth. In particular, since from the IASPEI-91 tables $\tilde{t}_0\,(h = 10\,\text{km}) - \tilde{t}_0\,(h = 0\,\text{km}) \approx$ 1.5 seconds and the

measured variability of $t_0(\mathrm{S}-\mathrm{P}) - \tilde{t}_0(h = 0 \text{ km})$ for well-located events recorded at calibrated regional stations is on the order of ± 3.5 seconds, we have assumed for preliminary analysis purposes that differences of $t_0(\mathrm{S}-\mathrm{P}) - \tilde{t}_0(h = 0 \text{ km})$ greater than about 5 seconds provide high confidence that the event depth is greater than 10 km and, consequently, that the event can be confidently screened out as a natural earthquake source.

We are currently evaluating this hypothesis test using regional data recorded from events in the source regions of Figure 2-11 for which the event depths have been well constrained by validated depth phase observations. For this application, P and S arrival times were determined at selected regional stations for well located REB events and the resulting $t_P - t_0$ and $t_S - t_P$ time intervals were used to evaluate the calibration constant in equation 4-4, where t_0 denotes the origin time from the well constrained hypocenter solution. Origin times for events recorded at each calibrated station were then estimated from observed $t_S - t_P$ intervals and compared with corresponding constrained teleseismic origin time estimates, $\tilde{t}_0(h=0\,\text{km})$, to test for significant focal depth. This process is illustrated for a sample of Honshu events recorded at station MJAR in Figure 4-4, where the determination of the calibration constant (left) and its application in a focal depth hypothesis test (right) are shown. It can be seen that, in this case, almost all the events with validated focal depths of greater than 50 km can be screened out as being too deep to be explosions with high confidence. The dashed line in the right-hand panel of this figure denotes the value of $\tilde{t}_0(h) - \tilde{t}_0(h=0\,\text{km})$ predicted as a function of focal depth by the teleseismic IASPEI-91 travel-time values, and it can be seen that the observed data show some systematic deviations from this relation that may indicate

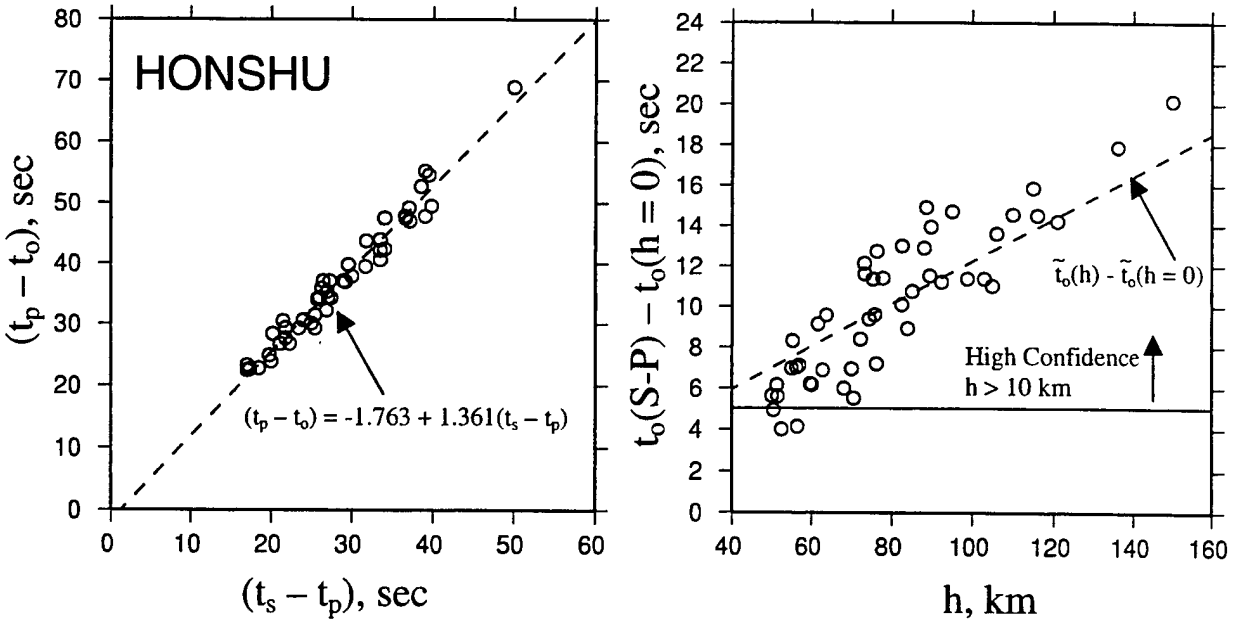

Figure 4-4. Application of the S-P origin time hypothesis test to data recorded from selected Honshu events at regional station MJAR ($\bar{\Delta} \approx 1.9°$).

variations in the regional station calibration constant as a function of epicentral distance and focal depth that will need to be further evaluated. In any case, this hypothesis test clearly shows promise for applications to event screening based on focal depth. The corresponding calibration results for the Hokkaido region of Japan are shown in Figure 4-5 where again, almost all events with validated depths of greater than 50 km are screened out as being to deep to be explosions with high confidence. In this case, the Hokkaido points in the right hand plot show larger scatter relative to the IASPEI prediction. This could be due to variation in the paths sampled or errors in the S or P arrival time picks, areas currently under investigation. Finally, the calibration results for station NIL for events in the Hindu Kush region of Asia are shown in Figure 4-6. Once again, all events are screened out as being to deep to be explosions, and here the data in the right-hand plot more closely follow the trend predicted by the simple, IASPEI earth model.

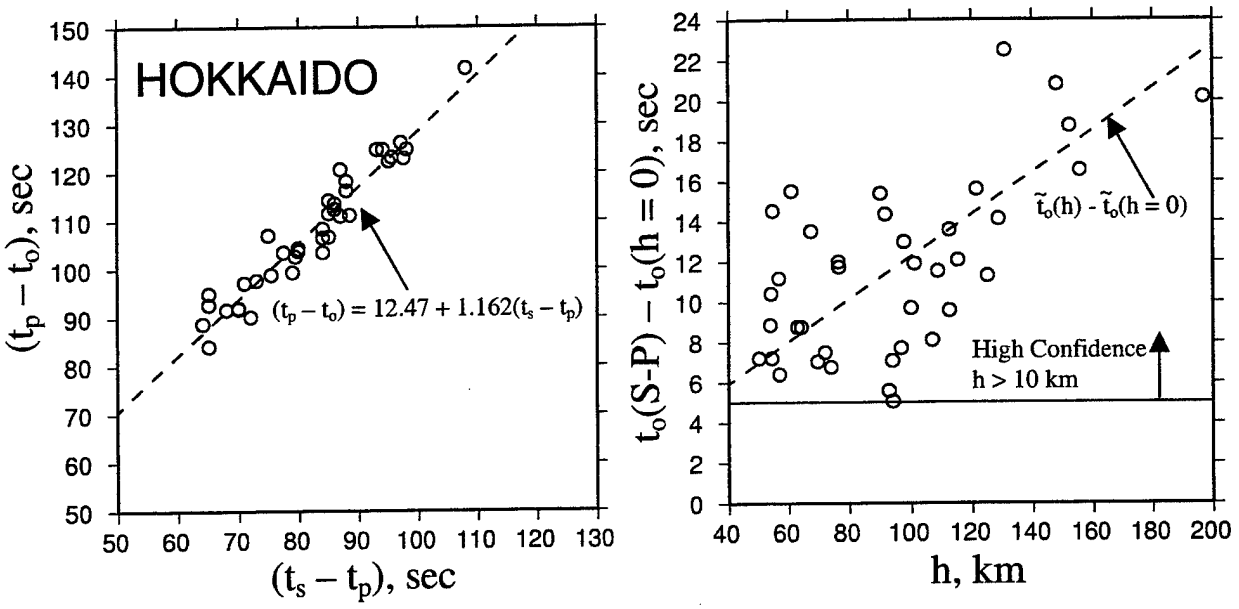

Figure 4-5. Application of the S-P origin time hypothesis test to data recorded from selected Hokkaido events at regional station MJAR ($\bar{\Delta} \approx 7.6°$).

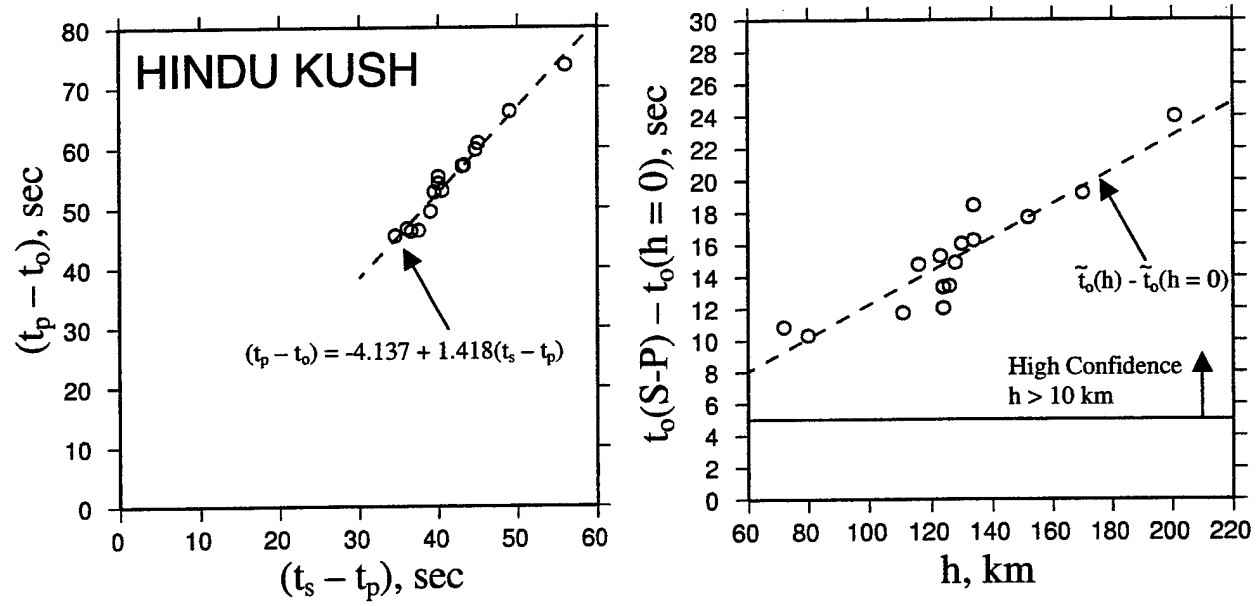

Figure 4-6. Application of the S-P origin time hypothesis test to data recorded from selected Hindu Kush events at regional station NIL ($\bar{\Delta} \approx 4.7°$).

The stability of the S-P calibration procedure can be evaluated by examining events for which we have obtained absolute, independent knowledge of the event depths and origin times. In this regard, we have collected P and S arrival time information from a large sample of PNE explosions recorded at station BRV, where the event depths and origin times are accurately known. Figure 4-7 shows the calibration curve (left) and associated errors in S-P origin time estimates (right), where these errors are calculated with respect to the known explosion origin times. Here we can see that the explosion data appear to show larger scatter than that seen in the earthquake data. This could be due to a greater variation in the travel paths for the explosions relative to the earthquakes for these widely dispersed PNE events, as well as the generally weak S wave onsets observed from explosion sources.

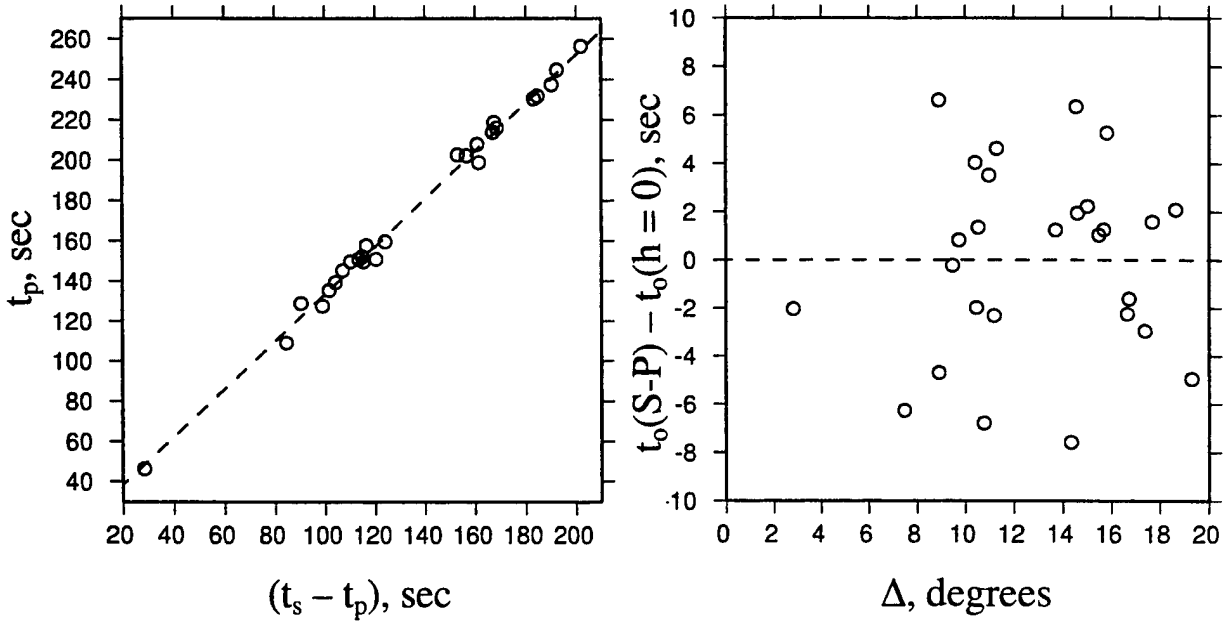

Figure 4-7. Calibration curve (left) and associated errors in S-P origin time estimates (right) obtained for Soviet PNE events recorded at Borovoye.

Figure 4-8 shows the errors in the S-P origin time estimates as a function of event location around Borovoye. It can be seen here that the travel paths sampled by these Borovoye recordings cover a broad geographic area. However, this figure also shows that there does not appear to be any correlation between the size and sign of the origin time residuals and the event locations.

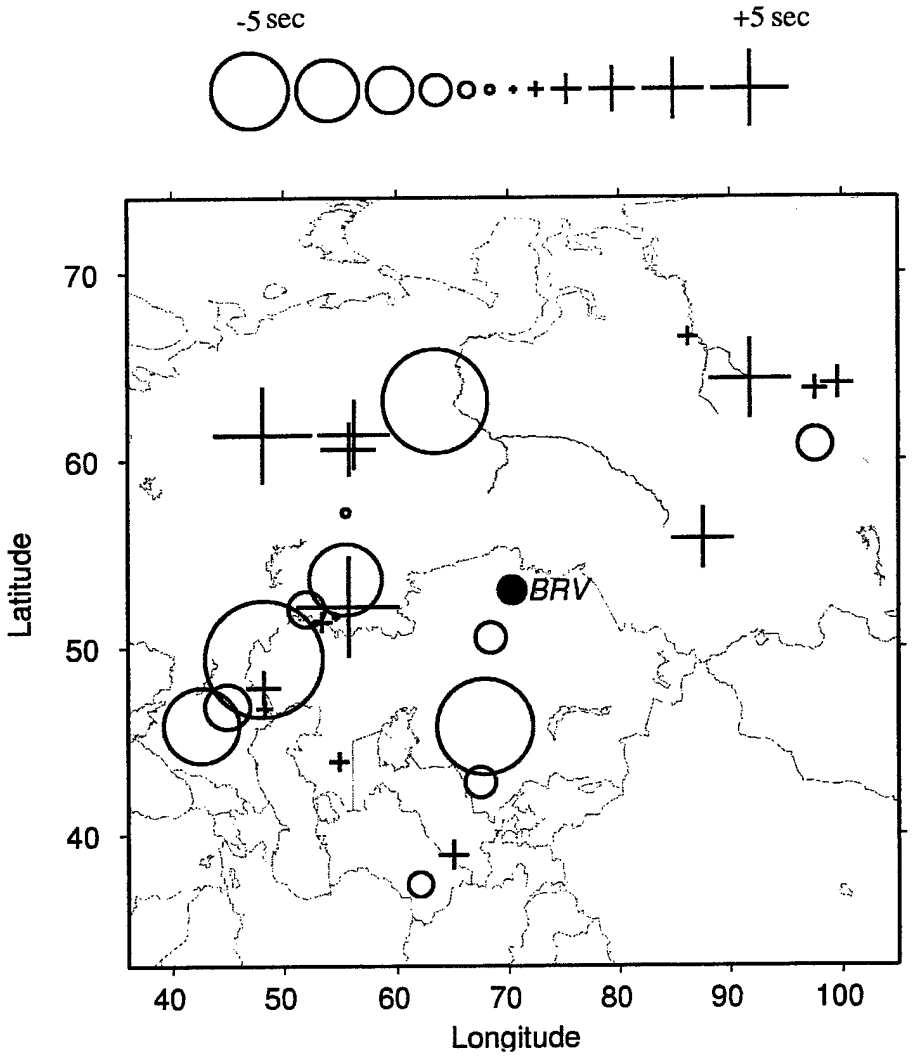

Figure 4-8. S-P origin time residuals as a function of event location for PNE's recorded at station BRV.

Clearly, this method of independently constraining the event origin time shows promise, in that it enables us to screen out events as having been too deep to be explosions in the absence of any depth phase information. It might also be used as a supplemental check on the validity of depth phase picks when the move-out of the picks is small or there is large uncertainty in our confidence of the depth phase picks. We are continuing to collect additional regional data from well located events in an attempt to evaluate the reliability of this origin time constraint and to determine its dependence on source location and depth. We are also investigating how best to incorporate this S-P calibration information into a more formal computation of focal depth uncertainty.

SECTION 5
SUMMARY AND CONCLUSIONS

This report has provided a summary of the results of a research program that has been directed toward the development of improved procedures for estimating focal depths of seismic sources for use in the monitoring of underground nuclear explosions. In particular, new analyst tools have been implemented and tested in an attempt to increase the detection and identification of the depth phases pP and sP, and a method of obtaining independent estimates of event origin time through the use of differential S-P arrival times has been investigated.

The detection and identification of the secondary depth phases pP and sP were addressed in Section 2, where a number of examples were presented to illustrate the effects of complicating factors such as the relative frequency content of pP and sP with respect to P, earthquake focal mechanism and the occurrence of anomalous P phases which are not predicted by the global travel time tables. A fully automatic network beamforming algorithm was then described for stacking raw IMS detection data to more consistently identify candidate depth phases for subsequent review by the IDC analyst. This new procedure has been tested and evaluated using data recorded from selected events in the Pamir-Hindu Kush, Hokkaido and central Honshu seismic zones as well as on events located near the Chinese explosion test site at Lop Nor. This algorithm has been integrated into the Analyst Review Station which is employed at both the U.S. NDC and the IDC and can now be tested using the full-processing environment of the representative nuclear monitoring systems.

In Section 3 we investigated the usefulness of the F detector and other tools for validating candidate depth phases identified by our network beamforming algorithm. That is, the presence of a prominent peak on a network detection stack does not, by itself, constitute a positive identification which is confident enough to be used for purposes of event identification. Rather, it identifies possible depth phases which have to be validated by further review and testing. We showed that the development, implementation and testing of improved analyst tools and quantitative tests will play a key role in the development of any new depth phase identification system.

A brief description of focal depth estimation determined from P wave first arrival times alone was presented in Section 4, where we describe a method of determining independent event origin times using regional S and P arrival time information. Specifically, it was shown that if S-P differential arrival time information is available from well-calibrated regional stations, it can be used to provide useful, independent estimates of the event origin time for use as constraints in the hypocenter location process. This method was applied to a series of well-located events from the Hindu Kush region and the Hokkaido and Honshu regions of Japan with promising results.

The research summarized above supports the following conclusions regarding seismic determination of focal depth:

(1) Analyst detection and identification of the depth phases pP and sP is complicated by the effects of earthquake focal mechanism and a variety of other factors. As a result, depth phase data were reported for only about 5% of the REB events analyzed during the GSETT-3 experiment.

(2) A new, automatic processing algorithm based on network beamforming of raw IMS detection data has been developed which has been shown to identify significant numbers of candidate depth phases which were not detected by the PIDC analysts. Application of this algorithm to data from a large sample of earthquakes from the Lop Nor, Pamir-Hindu Kush, Hokkaido and central Honshu seismic zones resulted in the identification of prominent candidate depth phase peaks near the published REB depth for over 70% of the events analyzed, including some with magnitudes as low as m_b=3.75 and depths as shallow as 18 km. This algorithm has been integrated into the Analyst Review Station (ARS) software which is employed at both the U.S. NDC and the IDC, and can now be evaluated using the full-processing environment of the representative nuclear monitoring systems as well as historical data archives.

(3) Preliminary applications of the F detector algorithm to the confirmation of depth phase identification have been encouraging and suggest that it could be used in conjunction with the network beamforming algorithm to provide analysts with a much improved capability to confidently identify more pP and sP arrivals.

(4) Analyses of focal depth estimates determined using P wave first arrival times alone indicate that there are a number of sources of systematic error which are not accounted for by existing hypocentral inversion codes and which can lead to significant bias in estimated focal depths and their associated uncertainty bounds. This shortcoming seriously limits the current applicability of estimated focal depth to nuclear monitoring. However, we have shown that if S-P differential arrival time information is available from well-calibrated regional stations, it can be used to provide useful, independent estimates of the event origin time for use as constraints in the hypocenter location process. That is, this method of independently constraining the event origin time could

be used to confidently screen out events as having been too deep to be explosions in the absence of any depth phase information.

REFERENCES

Blandford, R. R. (1974), An Automatic Event Detector at the Tonto Forest Seismic Observatory, *Geophysics*, **39**, 633 – 643.

Israelsson, H. (1994), "Stacking of Waveforms for Depth Estimation," *Center for Seismic Studies Final Report C94-02*.

Kind, R. and D. Seidl (1982), "Analysis of Broadband Seismograms From the Chile-Peru Area," *Bull. Seism. Soc. Am.*, **72**, pp. 2131-2145.

Murphy, J. R, R. W. Cook and B. W. Barker (2000), "Improved Focal Depth Determination For Use in Seismic Monitoring of Underground Nuclear Explosions", MSD-DFR-00-16621.

Pearce, R. G. (1977), "Fault Plane Solutions Using Relative Amplitudes of P and pP," *Geophys. J. R. Astron. Soc.*, **50**, 381-394.

Pearce, R. G. (1980), "Fault Plane Solutions Using Relative Amplitudes of P and Surface Reflections: Further Studies," *Geophys. J. R. Astron. Soc.*, **60**, 459-487.

Woodgold, C. R. D. (1999), "Wide Aperture Beamforming of Depth Phases by Timescale Contraction," *Bull. Seism. Soc. Am.*, **89**, pp. 165-177.

Woodward, R. L and R. G. North (2002). A Support System for Nuclear Explosion Monitoring Research and Development, *24th Seismic Research Review*, Ponte Vedra Beach, 906-914.